REVIEW ARTICLES

Optical properties of thin films

OPTICAL PROPERTIES OF THIN FILMS

By O. S. HEAVENS
Royal Holloway College, Englefield Green, Surrey

CONTENTS

Abstract. The optical behaviour of a surface carrying a transition layer is discussed, as a problem in scattering. The results are given of the application of electromagnetic theory to the case of a single parallel-sided film. Methods are given for extending this treatment to the case of multiple parallel-sided layers. Both analytical and graphical solutions are considered. Features governing the design of certain multilayer systems are given. A survey is made of the many methods now available for the determination of the thickness and optical constants of materials in the form of thin films. The range, accuracy and conditions of application of the various methods are summarized. A selection of the results obtained on a range of metallic and dielectric films is made and the basis of interpretation of these results is given. It is shown that the apparently anomalous variations of the optical constants of metal films with film thickness can be attributed to the granular nature of such films. Although less spectacular variations are observed in the properties of dielectric films, it is seen that for some materials the optical behaviour suggests the presence of marked inhomogeneity and anisotropy. Films formed chemically and electrolytically are briefly mentioned.

Recent methods of controlling the thickness of films during deposition are given, together with a selection of the more important applications of thin films in optics. These include anti-reflecting and high reflecting systems, narrow-band, wide-band and cut-on multilayer filters, the use of thin films in polarizing systems and the application of thin films in heat-absorbing systems.

§ 1. Introduction

The optical behaviour of thin films may be considered from two viewpoints. From studies of the structures of the films formed by most available methods it is found that films generally consist of aggregates of crystallites of variable size and orientation and with differing extents of voids. Description of the optical behaviour of such a sytsem is essentially a scattering problem and this approach is often used in studying the effects of, for example, a transition layer on the surface of a solid. The mathematical problems involved are difficult generally but become tractable for layers whose thickness is of the order of molecular spacings.

It proves convenient to treat problems involving thicker layers—e.g. tens of millimicrons upwards—by describing the layer by a refractive index and, for absorbing materials, by an extinction coefficient. The optical properties of the layer can then be calculated using the classical electromagnetic theory. No difficulty arises in extending this approach to systems of multiple films: the reflectance and transmittance can be calculated explicitly in terms of the optical constants and film thicknesses. The mathematics is straightforward although cumbersome: problems are readily handled by digital computers or graphical methods may be found useful. The experimentally observed properties of films of some materials are found to agree closely with the predictions of electromagnetic theory, thus validating this approach to the film problem. For layers of thickness

of the order of molecular dimensions, however, scattering theory shows that such films cannot be described in terms of a refractive index and extinction coefficient. In cases where discrepancies are found for thick films these may be generally attributed to a lack of homogeneity of the film arising from, for instance, a change in film structure with film thickness. It is sometimes possible to deduce from the optical examination information on the film structure.

A wealth of methods has by now been developed for the measurement of the thickness and optical constants of films. Provided that the films are smooth and lie on a smooth substrate, interferometric and photometric methods enable a precision of better than 1 mμ to be attained. For transparent films the refractive index is directly measurable to within $\pm 0{\cdot}002$ under favourable conditions. The optical constants of absorbing films are generally rather more difficult to determine accurately : an accuracy to about 2% may be reached with existing methods. In the case of measurements on evaporated metal films, the sensitivity of the optical constants to conditions of preparation is so great that no higher accuracy in the optical measurement is at present called for.

With the increasing wide application of films in optical devices, methods of monitoring film thickness have been developed to an impressive standard. For the construction of multilayer filters of sophisticated design the precision of thickness control now attainable enables filters with (literally) scores of layers to be made. As more and more materials suitable for use in multilayer systems are discovered we move steadily towards the time when filters will be tailor-made for (almost) any desired purpose. No attempt is made in § 8 to give a comprehensive list of applications of thin films in optics : the examples discussed may be considered typical of the uses to which thin films may be put.

§ 2. Reflection of Light at a Single Surface

2.1. *Calculation of Effect of Surface Layer*

With the aid of electromagnetic theory the calculation of the reflectance and state of polarization of light reflected from the plane surface separating two homogeneous media is straightforward. The media are assumed to be continua and are described by refractive indices and, in the case of absorbing media, extinction coefficients. If visible light is considered, the assumption of a continuous medium is reasonably justified since the wavelengths entailed are some thousand times greater than the separations between atoms. For the case of reflection at the plane surface of an isotropic, homogeneous, non-absorbing medium of refractive index n, we obtain for the amplitude reflection coefficients r_p (electric vector $\parallel$ plane of incidence) and r_s (electric vector $\perp$ plane of incidence) :

$$r_p = -\frac{\tan(\phi_0-\phi_1)}{\tan(\phi_0+\phi_1)} \qquad \ldots\ldots(1)$$

$$r_s = +\frac{\sin(\phi_0-\phi_1)}{\sin(\phi_0+\phi_1)} \qquad \ldots\ldots(2)$$

where ϕ_1, ϕ_0 are the angles of incidence and refraction respectively. The sign convention is that used by Ditchburn (1952). The difference between the phase

changes on reflection $\delta = \delta_p - \delta_s$ undergoes an abrupt change at the polarizing angle ϕ_p, this being defined as the angle of incidence at which $\phi_0 + \phi_1 = \frac{1}{2}\pi$. Figure 1 shows the calculated dependence of δ on angle of incidence together with a typical experimental curve. The lack of sharpness of the experimentally observed change of δ with ϕ_1 is ascribed to a transition layer at the surface. This may arise from, for instance, the action of polishing, the presence of contamination or effects of surface tension on the atomic arrangement near the surface. Since the sensitivity attainable by standard polarimetric techniques is high, very small departures from the theoretical prediction for the homogeneous solid can be detected. Such methods therefore provide a powerful means of studying surface films, provided the observations can be correctly interpreted.

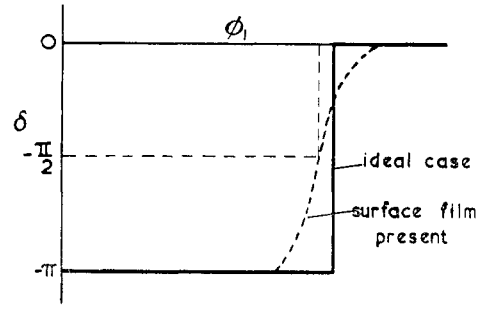

Figure 1. Dependence of δ on angle of incidence ϕ.

The effect of a continuous variation of the optical properties of a surface layer on the state of reflected light was treated by Drude (1891) and McLaurin (1905). Strachan (1933) treated the case of a two-dimensional distribution of dipoles on a surface, obtaining expressions for the reflection coefficients and phase changes in terms of three scattering coefficients, defined as the components of the strengths of the Hertzian dipoles produced at the surface of the medium by the electric field of the incident wave. The results are not too intractable for an isotropic film. Considerable simplification is effected by the treatment of Sivukhin (1956) in which it is shown that the effect of a transition layer of any thickness can be reduced to that of two infinitesimally thin layers with dipole moment surface densities. For a transition layer of thickness small compared with the wavelength of the light used, the problem reduces to that of considering a single surface dipole moment distribution.

The treatment is restricted to the calculation of the intensities of reflected waves at distances large compared with the intermolecular distances in the medium. That this approximation is entirely satisfactory is shown by Ewald (1916): the radiation field from a crystal lattice is found to be practically equal to that for a continuous medium even at distances from the surface of the order of the lattice constant of the crystal.

For a plane monochromatic wave incident on the surface of the medium, the polarization in the medium may be written:

$$\mathbf{P} = \mathbf{P}_0 \exp i(\omega t - \kappa r). \qquad \ldots\ldots(3)$$

The effect of a thin transition layer (thickness $\ll \lambda$) may be expressed in terms of a supplementary dipole moment per unit area of surface, given by

$$\tau = \tau_0 \exp i(\omega t - \kappa_x x) \qquad \ldots\ldots(4)$$

where Oz is normal to the surface and $y = 0$ is the plane of incidence. If it is assumed that the supplementary polarization at the surface is small compared with the polarization in the absence of the transition layer, then the results for the reflection coefficients may be expressed in terms of parameters γ_m $(m = x, y, z)$ given by

$$\gamma_m = \frac{\tau_{0m}}{P_{0m}}. \qquad \ldots\ldots(5)$$

The expressions for the reflection coefficients r_p and r_s may then be written

$$r_p = -\frac{\tan(\phi_0 - \phi_1)}{\tan(\phi_0 + \phi_1)}\left[1 + 2if\cos\phi_0 \frac{\gamma_x \cos^2\phi_1 - \gamma_z \sin^2\phi_0}{\cos^2\phi_1 - \sin^2\phi_0}\right] \qquad \ldots\ldots(6)$$

and

$$r_s = \frac{\sin(\phi_0 - \phi_1)}{\sin(\phi_0 + \phi_1)}[1 + 2if\gamma_y \cos\phi_0]. \qquad \ldots\ldots(7)$$

f is the magnitude of the wave vector of the incident wave. For an isotropic surface distribution, $\gamma_x = \gamma_y$.

The results given above are obtained from a first-order approximation based on the assumptions stated. It is shown (Sivukhin 1956) that in taking approximation to the second order, it is necessary to consider quadrupole radiation from the transition layer. In principle if the molecular structure of the surface is known, the parameters γ_m (and also the further parameters of the second-order approximation) are calculable.

An interesting result of the first-order theory, and one which does not appear to have been put to experimental test, is that the ellipticity of the light reflected from a surface covered by a transition layer should be inversely proportional to the wavelength of the radiation used. A further conclusion is that a transition can be characterized phenomenologically by a refractive index only if its thickness is large compared with molecular dimensions. Under this condition, the first-order Sivukhin equations reduce to those of Drude whilst the second-order equations yield the McLaurin results.

2.2. *Experimental Results*

Experimental investigation of the transition layer on the surfaces of solids suffers from the difficulty that, in order that accurate measurements can be made, an optically smooth, flat surface is required. There appears to be no way of producing such a surface without using a method which is liable to produce surface disorder. Measurements of the differential phase change on (total) reflection at a glass prism face (Ditchburn and Orchard 1954) show large differences from the value calculated from the (bulk) refractive index, even for a range of different surface treatments. The effect of repolishing the surface was to yield results corresponding to a transition layer about 10 mμ thick. Measurements by the same authors on light totally reflected from a flowing water surface were found to agree closely with the predictions of simple theory, suggesting that the results obtained

on solids may well arise from unavoidable surface disorder. The effect of surface tension forces may still, however, cause departures from simple theory in the case of a solid since the estimated surface tensions in solids are 1–2 orders of magnitude higher than those observed in liquids.

§ 3. Optical Behaviour of a Single Film

3.1. *General*

Much interest has centred in recent years on films, or systems of films, of thickness comparable with the wavelengths of visible light. The practice of coating lenses with a quarter-wave anti-reflecting (blooming) layer is now common. If multiple reflections are neglected, it is a trivial calculation to show that, for complete extinction at a given wavelength, the refractive index of the anti-reflecting layer n_a must equal the square root of the substrate index. In fact, this result is still correct if the effect of multiple reflections is included. Practical difficulties prevent the easy realization of the index required for coating a typical crown glass. The low index needed can be achieved only by arranging that the film be full of holes : the mechanical properties of such films are unsatisfactory. Magnesium fluoride is widely used : although its index is higher than the optimum, it may be deposited as a very hard, stable, durable film. Results of recent studies of the properties of MgF_2 are given in § 6.2.

3.2. *Reflection and Transmission at a Single Film*

Expressions for the reflection and transmission coefficients of a surface covered with a single homogeneous isotropic film are conveniently expressed in terms of the Fresnel reflection and transmission coefficients for the two interfaces. These quantities may conveniently be defined here in general terms since they are needed for the treatment of multiple layers in § 4. The Fresnel coefficients (ratio of reflected or transmitted to incident amplitude) depend on the plane of polarization considered. For light incident from a medium of refractive index n_m on the boundary with a medium of index n_{m-1} we have (figure 2) for the p-component†

$$r_{mp} = \frac{n_m \cos\phi_{m-1} - n_{m-1}\cos\phi_m}{n_m \cos\phi_{m-1} + n_{m-1}\cos\phi_m} \quad \text{(reflection)} \qquad \ldots\ldots(8)$$

$$t_{mp} = \frac{2n_m \cos\phi_m}{n_m \cos\phi_{m-1} + n_{m-1}\cos\phi_m} \quad \text{(transmission).} \qquad \ldots\ldots(9)$$

For the s-component

$$r_{ms} = \frac{n_m \cos\phi_m - n_{m-1}\cos\phi_{m-1}}{n_m \cos\phi_m + n_{m-1}\cos\phi_{m-1}} \qquad \ldots\ldots(10)$$

$$t_{ms} = \frac{2n_m \cos\phi_m}{n_m \cos\phi_m + n_{m-1}\cos\phi_{m-1}}. \qquad \ldots\ldots(11)$$

The ϕ's are related by Snell's law :

$$n_m \sin\phi_m = n_{m-1}\sin\phi_{m-1}. \qquad \ldots\ldots(12)$$

† The definitions given here for Fresnel coefficients differ from those quoted in some publications (e.g. Abelès 1948 a, Heavens 1955). The reason is simply that, for some treatments of the multi-layer problem, it proves more convenient to label the substrate n_0 and number the films upwards from the substrate. In order that the notation for various treatments given below shall be unified, this system will be adopted throughout.

In order to simplify the equations, Fresnel coefficients will generally be written simply as r_m, t_m, with the understanding that when (8) and (9) are used, the result gives the p-component and, with (10) and (11), the s-component.

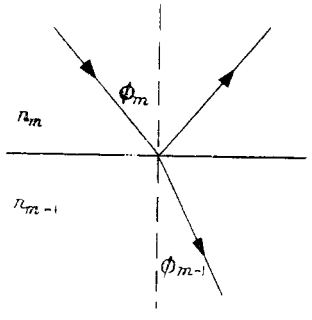

Figure 2.

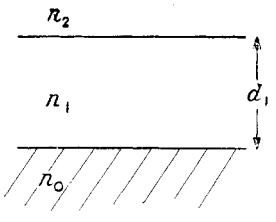

Figure 3. Single film.

For a single film of index n_1 and thickness d_1 on a substrate of index n_0 (figure 3), the amplitude reflection and transmission coefficients are given by

$$R = \frac{r_2 + r_1 \exp(-2i\delta_1)}{1 + r_1 r_2 \exp(-2i\delta_1)} \qquad \ldots\ldots(13)$$

$$T = \frac{t_1 t_2 \exp(-i\delta_1)}{1 + r_1 r_2 \exp(-2i\delta_1)} \qquad \ldots\ldots(14)$$

where
$$\delta_1 = 2\pi\nu n_1 d_1 \cos\phi_1 \qquad \ldots\ldots(15)$$

and
$$\nu = 1/\lambda.$$

These results follow simply and directly from summation of multiple beams in the film. For non-normal incidence equations (13) and (14) each yield two equations, corresponding to each plane of polarization.

The energies crossing unit area per second normal to the reflected and transmitted beams are given by $n_0 RR^*$ and $n_2 TT^*$. Hence the reflectance of the system is given by

$$\mathbf{R} = RR^* = \frac{r_1^2 + 2r_1 r_2 \cos 2\delta_1 + r_2^2}{1 + 2r_1 r_2 \cos 2\delta_1 + r_1^2 r_2^2}. \qquad \ldots\ldots(16)$$

If the transmittance $\mathbf{T}$ is defined as the ratio of illumination on screens perpendicular to the transmitted and incident beams, then

$$\mathbf{T} = \frac{n_2}{n_0} TT^* = \frac{n_2}{n_0} \frac{t_1^2 t_2^2}{1 + 2r_1 r_2 \cos 2\delta_1 + r_1^2 r_2^2}. \qquad \ldots\ldots(17)$$

We may note that the transmission characteristic may equally well be defined by the ratio of the total flux transmitted by unit area of the film to that incident (Weinstein 1954) in which case the transmittance $\mathbf{T}_f$ would be

$$\mathbf{T}_f = \frac{n_2 \cos\phi_2}{n_0 \cos\phi_0} \frac{t_1^2 t_2^2}{1 + 2r_1 r_2 \cos 2\delta_1 + r_1^2 r_2^2}. \qquad \ldots\ldots(18)$$

For the case of normal incidence, $\mathbf{T} = \mathbf{T}_f$.

3.3. *Normal Incidence : Non-absorbing Media*

Equations (16) and (17) may be written directly in terms of the refractive indices of the media. The Fresnel coefficients are equal for both planes of polarization, and are given by

$$r_1 = \frac{n_1 - n_0}{n_1 + n_0}, \quad t_1 = \frac{2n_1}{n_1 + n_0}, \qquad \ldots\ldots(19)$$

$$r_2 = \frac{n_2 - n_1}{n_2 + n_1}, \quad t_2 = \frac{2n_2}{n_2 + n_1}. \qquad \ldots\ldots(20)$$

For this case

$$\mathbf{R} = \frac{(n_0^2 + n_1^2)(n_1^2 + n_2^2) - 4n_0 n_1^2 n_2 + (n_0^2 - n_1^2)(n_1^2 - n_2^2)\cos 2\delta_1}{(n_0^2 + n_1^2)(n_1^2 + n_2^2) + 4n_0 n_1^2 n_2 + (n_0^2 - n_1^2)(n_1^2 - n_2^2)\cos 2\delta_1} \qquad \ldots\ldots(21)$$

$$\mathbf{T} = \frac{8n_0 n_1^2 n_2}{(n_0^2 + n_1^2)(n_1^2 + n_2^2) + 4n_0 n_1^2 n_2 + (n_0^2 - n_1^2)(n_1^2 - n_2^2)\cos 2\delta_1}. \qquad \ldots\ldots(22)$$

These equations are seen to be symmetrical with respect to n_0 and n_2, showing that the values of reflectance and transmittance given above apply for light incident from either side of the film.

Equation (22) gives the intensity of the beam in the substrate medium n_0. If the light emerges from the back of the substrate medium, then allowance must be made for any reflection effect at the surface of emergence. If the substrate is a parallel-sided slab, multiple reflections must be considered. If the substrate thickness is large, so that multiply reflected beams are incoherent, intensities are added. If the substrate thickness is small, so that the beams are coherent then the system becomes a two-film system and the treatment of § 3 must be used.

Equations (13) and (14) may still be used for the case of absorbing media : the values of n used in evaluating the Fresnel coefficients and in the δ_1 term are replaced by a complex $\mathbf{n} \equiv n - ik$ where k is the extinction coefficient. The values of ϕ_1 obtained from Snell's law are complex, a manifestation of the fact that, in an absorbing medium, the planes of constant amplitude may be inclined to the planes of constant phase of the wave.

The determination of optical constants of an absorbing film from reflection and transmission data, using a digital computer, is described by Harris and Loeb (1955).

3.4. *Anisotropic and Absorbing Media*

The case of an anisotropic, absorbing film sandwiched between transparent isotropic media has been dealt with by Schopper (1952 a). The more general case in which any or all of the three media are anisotropic and absorbing has been treated by Bousquet (1957) in the following way.

It is first necessary to evaluate the Fresnel coefficients for the case of reflection and transmission at the interface between two such media. For the coordinate system shown in figure 4 we may write for the phase terms of the electric vectors of the incident, reflected and refracted waves :

$$\exp i\omega(t - \alpha_1 x - \gamma_1 z), \quad \exp i\omega(t - \alpha_1 x + \gamma_1 z)$$

and

$$\exp i\omega(t - \alpha_2 x - \gamma_2 z).$$

For an isotropic, non-absorbing system, $\alpha_i = (n_i \sin\phi_i)/c$ and $\gamma_i = (n_i \cos\phi_i)/c$ where $i = 1, 2$ and ϕ is the angle of incidence. For the general case, the value of n_i appropriate to the direction of propagation must be inserted. Bousquet's treatment is restricted to the case in which the normal to the surface is a privileged direction of the crystal. It is then possible to express the propagation terms

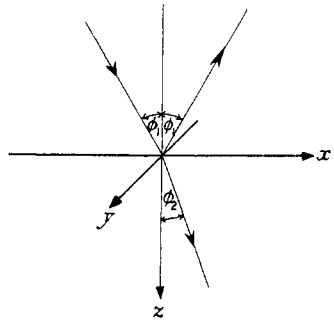

Figure 4.

α and γ quite simply in terms of the principal dielectric constants $\epsilon_x, \epsilon_y, \epsilon_z$. For absorbing media these are complex. The Fresnel coefficients may be written

(i) Electric vector $\perp$ plane of incidence

$$r_{1p} = \frac{\gamma_1 - \gamma_0}{\gamma_1 + \gamma_0}, \quad t_{1p} = \frac{2\gamma_1}{\gamma_1 + \gamma_0} \qquad \ldots\ldots(23)$$

where

$$\gamma_0^2 = \frac{\epsilon_{y0}}{c^2} - \alpha_1^2. \qquad \ldots\ldots(23a)$$

(ii) Electric vector $\parallel$ plane of incidence

$$\left.\begin{aligned} r_{1s} &= \frac{\epsilon_{x1}\gamma_0 - \epsilon_{x0}\gamma_1}{\epsilon_{x1}\gamma_0 + \epsilon_{x0}\gamma_1} \\ t_{1s} &= \frac{2\gamma_1/\epsilon_{x1}}{(\gamma_1/\epsilon_{x1} + \gamma_0/\epsilon_{x0})} \end{aligned}\right\} \qquad \ldots\ldots(24)$$

where

$$\gamma_0^2 = \frac{\epsilon_{x0}}{c^2} - \alpha_1^2 \frac{\epsilon_{x0}}{\epsilon_{z0}}. \qquad \ldots\ldots(24a)$$

The values of r_{1p}, t_{1p} and r_{1s}, t_{1s} may thus be obtained in terms of the direction of the incident beam and of the dielectric constants of the media. Expressions for $r_{2p}, t_{2p}, r_{2s}, t_{2s}$ for the case of incidence from medium 2 to medium 1 may be written down by inspection from equations (23) and (24). The amplitude reflection coefficients for the case of a film of thickness d_1 are then obtained from

$$R = \frac{r_2 + r_1 \exp(-2i\omega\gamma_1 d_1)}{1 + r_1 r_2 \exp(-2i\omega\gamma_1 d_1)} \qquad \ldots\ldots(25)$$

$$T = \frac{t_1 t_2 \exp[-i\omega d_1(\gamma_1 - \gamma_2)]}{1 + r_1 r_2 \exp(-2i\omega\gamma_1 d_1)} \qquad \ldots\ldots(26)$$

where values of r, t appropriate either to the p- or s-components of polarization are inserted. With the help of equations (23*a*) and (24*a*), together with their

counterparts for the 2–3 interface, R and T may be calculated in terms of (α_2, γ_2) and the parameters of the media. For absorbing media, the explicit expressions are cumbersome : the computation is best done stepwise.

§ 4. Multilayer Theory

4.1. *Methods of Calculation*

Calculation of the reflectance and transmittance of a system of parallel-sided films has been effected in a number of ways. Crook (1948) has extended the method of summing multiply reflected beams, which yields the result for a single film easily, to the case of two films and has outlined the form of procedure for

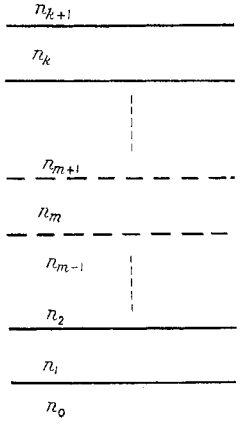

Figure 5. Notation for multilayer system.

expressing the result for n layers in terms of that for $n-1$ layers. The process is however cumbersome and not convenient for computation. Rouard (1937) and Vašíček (1950) make use of the fact that, since a single film may be characterized by an effective reflection coefficient and phase change, then such a film may be replaced, for the purpose of computing reflectances, by a single surface with these properties. By a stepwise procedure, one can work through the whole system of layers until the final boundary is reached. For a system of k layers on a substrate of index n_0 (figure 5), the amplitude reflection coefficient for the first film may be written

$$\rho_2 \exp(i\Delta_2) = \frac{r_2 + r_1 \exp(-2i\delta_1)}{1 + r_1 r_2 \exp(-2i\delta_1)} \qquad \ldots\ldots(27)$$

where r_2, r_1 are the Fresnel coefficients for the n_2/n_1 and n_1/n_0 interfaces respectively. The reflection coefficient for the first two films may then be written

$$\rho_3 \exp(i\Delta_3) = \frac{r_3 + \rho_2 \exp(i\Delta_2) \exp(-2i\delta_1)}{1 + r_3 \rho_2 \exp(i\Delta_2) \exp(-2i\delta_1)}. \qquad \ldots\ldots(28)$$

Thus $\rho_4, \Delta_4, \rho_5, \Delta_5, \ldots \rho_{k+1}, \Delta_{k+1}$ are determined successively. The amplitude reflection coefficient for the whole system of films is ρ_{k+1}, so the reflectance is simply $\rho_{k+1}{}^2$. The extension to the case of absorbing layers simply entails replacing the real indices n by complex values $n - ik$ in the expressions for r and δ. It should

be noted however that the simple concept of multiple reflections in an absorbing layer forming part of the multilayer system may give rise to difficulties (Berning 1956).

A disadvantage of this method of calculation is that if the effect of altering the thickness or refractive index of any layer in the system is being studied, then the procedure given above must be repeated for all layers subsequent to the one changed. This drawback is avoided in the matrix method discussed below.

Some simplification results for the case of normal incidence and recurrence relations have been given by Godfrey (1957) which are convenient for obtaining some features of systems of practical importance.

For the system of figure 5, and for normal incidence, the amplitude reflection coefficient of the first m films may be written

$$\rho_m \exp(i\Delta_m) = \frac{n_{m+1} - N_m}{n_{m+1} + N_m} \qquad \ldots\ldots(29)$$

which serves to define N_m. Godfrey calls this the 'film index'—perhaps not a satisfactory name. The recurrence relation between N_{m-1} and N_m is readily seen to be

$$\frac{N_m - n_m}{N_m + n_m} = \frac{N_{m-1} - n_m}{N_{m-1} + n_m} \exp(-4\pi i \nu n_m d_m). \qquad \ldots\ldots(30)$$

For absorbing layers n_m is replaced by $\mathbf{n}_m \equiv n_m - ik_m$. If none of the layers is absorbing the reflectance and transmittance of the system of k layers are given by

$$\mathbf{R}_k = \left| \frac{n_{k+1} - N_k}{n_{k+1} + N_k} \right|^2 \qquad \ldots\ldots(31)$$

$$\mathbf{T}_k = \frac{4 n_0 n_{k+1}}{(n_1 + n_0)^2} \prod_1^k \left| \frac{N_m + n_m}{N_m + n_{m+1}} \right|^2. \qquad \ldots\ldots(32)$$

These expressions are particularly convenient for calculating the maximum reflectance of quarter-wave stacks. For this case the exponential term in equation (30) becomes unity, thus simplifying the recurrence relation for N_m, N_{m-1}. For an even number $2s$ of layers of the form LHL ... LH, the reflectance is given by

$$\mathbf{R}_{2s} = \left(\frac{n_0 f - n}{n_0 f + n} \right)^2 \qquad \ldots\ldots(33)$$

where $f = (n_H/n_L)^{2s}$ and n is the refractive index of the medium of incidence. For the system of $2s+1$ layers, HLH ... LH, the reflectance is

$$\mathbf{R}_{2s+1} = \left(\frac{f n_H^2 - n n_0}{f n_H^2 + n n_0} \right)^2. \qquad \ldots\ldots(34)$$

For high-reflecting stacks, in which the reflectance approaches unity, these may be written in the convenient approximate forms

$$\mathbf{R}_{2s} \simeq 1 - \frac{4n}{n_0 f}; \quad \mathbf{R}_{2s+1} \simeq 1 - \frac{4 n n_0}{n_H^2 f}. \qquad \ldots\ldots(35)$$

The special case in which the thicknesses of the layers forming a periodic multilayer system are small compared with the wavelength used has been dealt with by Vasilkovsky (1957). Such a system behaves as a single film with an

equivalent refractive index equal to the root-mean-square of the indices of the layers of the system. The accuracy of the calculations using the simplified formula improves as the ratio thickness/wavelength decreases. For semiconducting materials the simple formula is valid for thickness/wavelength not greater than 10^{-2}.

4.2. *Matrix Method of Solution*

The equations relating the amplitudes of the electric vectors in successive media can be conveniently written in matrix notation (Weinstein 1947, Herpin 1947, Abelès 1948 b, Muchmore 1948, Canals Frau 1952, Sukhanovsky 1956, Kard 1957 a). This form is generally the most convenient for computation either by hand or by digital computer.

If we denote by E^+_m the amplitude of the electric vector of the wave travelling in the direction of incidence in the mth layer and by E^-_m that of the negative-going wave, solution of the equations of propagation readily yields the following relations between $E^\pm_m$ and $E^\pm_{m-1}$:

$$\left.\begin{aligned} E^+_m &= t_m^{-1}[E^-_{m-1}\exp(i\delta_{m-1}) + r_m E^-_{m-1}\exp(-i\delta_{m-1})] \\ E^-_m &= t_m^{-1}[r_m E^+_{m-1}\exp(i\delta_{m-1}) + E^-_{m-1}\exp(-i\delta_{m-1})]. \end{aligned}\right\} \quad \ldots\ldots(36)$$

Where the r_m and t_m are given,† for whichever plane of polarization is considered, by equations (8) to (11).

Equation (36) may be written

$$\begin{aligned} \begin{pmatrix} E^+_m \\ E^-_m \end{pmatrix} &= \frac{1}{t_m}\begin{pmatrix} \exp(i\delta_{m-1}) & r_m\exp(-i\delta_{m-1}) \\ r_m\exp(i\delta_{m-1}) & \exp(-i\delta_{m-1}) \end{pmatrix}\begin{pmatrix} E^+_{m-1} \\ E^-_{m-1} \end{pmatrix} \\ &= \frac{1}{t_m} M_{m-1}\begin{pmatrix} E^+_{m-1} \\ E^-_{m-1} \end{pmatrix}. \end{aligned} \quad \ldots\ldots(37)$$

The solution for a stack of k layers on a substrate is thus given simply by

$$\begin{pmatrix} E^+_{k+1} \\ E^-_{k+1} \end{pmatrix} = \frac{M_k M_{k-1}\ldots M_2 M_1}{t_k t_{k-1}\ldots t_2 t_1}\begin{pmatrix} E^+_0 \\ E^-_0 \end{pmatrix} \quad \ldots\ldots(38)$$

from which the reflectance $\mathbf{R} = \dfrac{|E^-_{k+1}|^2}{|E^+_{k+1}|^2}$

is readily obtained. The transmittance $\mathbf{T}$ is given by

$$\left.\begin{aligned} &\text{p-component:} \quad \mathbf{T}_p = \frac{n_0}{n_{k+1}}\frac{|E^+_0|^2}{|E^+_{k+1}|^2} \\ &\text{s-component:} \quad \mathbf{T}_s = \frac{n_0\cos^2\phi_{k+1}}{n_{k+1}\cos^2\phi_0}\frac{|E^+_0|^2}{|E^+_{k+1}|^2}. \end{aligned}\right\} \quad \ldots\ldots(39)$$

The value of the transmittance defined in terms of light fluxes [equation (18)] is given, for both p- and s-components, by

$$\mathbf{T}_f = \frac{n_0\cos\phi_{k+1}}{n_{k+1}\cos\phi_0}\frac{|E^+_0|^2}{|E^+_{k+1}|^2}. \quad \ldots\ldots(40)$$

† We note the existence of needless confusion of notation here. Although the notation for Fresnel coefficients consistent with that given in equations (8)–(11) has been generally used (Cotton 1950, Malé 1950, Mayer 1950) the notation used by Weinstein (1954) differs, although not sufficiently to avoid the danger of confusion.

In evaluating the latter expression, however, the appropriate p- or s-values of Fresnel coefficients must be used.

An alternative form of recurrence relation may be obtained in terms of the components of **E** and **H**, giving

$$\begin{pmatrix} E_{m+1} \\ H_{m+1} \end{pmatrix} = \begin{pmatrix} \cos\delta_m & (i/u_m)\sin\delta_m \\ iu_m \sin\delta_m & \cos\delta_m \end{pmatrix} \begin{pmatrix} E_m \\ H_m \end{pmatrix} \qquad \ldots\ldots(41)$$

where $E_m = E^+{}_m + E^-{}_m, \quad H_m = u_m(E^+{}_m - E^-{}_m).$

For the p-component $u_m = n_m \cos\phi_m$ and for the s-component $u_m = n_m/\cos\phi_m$. One important advantage of this form of equation (41) as compared with equation (37) is that the square matrix of equation (41) contains only quantities characteristic of one layer of the system. The Fresnel coefficients in equation (37) depend on the indices of two media. It will be noted that the determinant of the square matrix is unity. Since the determinant of the product of any number of such matrices is also unity, the correctness of computation is easily checked at any stage. For non-absorbing films, the leading diagonal elements are real and the product determination straightforward. If absorbing films are present, then equation (41) offers no particular advantages over equation (36) for purposes of computation.

The development of experimental techniques in recent years enables systems of dozens of layers to be made without difficulty. Hand computation for such problems is entirely uneconomic. This type of computation is easily handled by an automatic digital computer, which can be programmed to deal with the problem more cheaply, more reliably and more accurately than by the use of human labour.

4.3. *Graphical Solutions of Multilayer Problems*

If the scale of work contemplated does not justify the programming of a computer, or if computer services are not available, there are several graphical methods available for dealing with multilayer problems (Malé 1950, Cotton 1950, Blaisse 1950, Krylova 1958). One of the best known is taken from the field of transmission lines, in which the Smith Chart (Kraus 1949) has long been in use. Using the variable $y_m = H_m/u_m E_m$ (known as the admittance), the recurrence relation for y is

$$y_{m+1} = \frac{u_m}{u_{m+1}} \frac{i\sin\delta_m + y_m \cos\delta_m}{\cos\delta_m + iy_m \sin\delta_m} \qquad \ldots\ldots(42)$$

which may be written in terms of the amplitude reflection coefficient

$$R_m = E^-{}_m/E^+{}_m$$

as

$$y_{m+1} = \frac{u_m}{u_{m+1}} \left(\frac{1 - R_m \exp(-2i\delta_m)}{1 + R_m \exp(-2i\delta_m)} \right). \qquad \ldots\ldots(43)$$

The coordinate mesh of the Smith Chart is that of the function y of the conformal transformation $y = (1-R)/(1+R)$ so the chart may be used to obtain R_{m+1} from R_m and hence, by successive use, the amplitude reflection coefficient for the whole system.

A slightly more convenient form of graphical calculator is that of Kard (1956). For the interface between the $(m+1)$th and mth layers, the amplitude reflection coefficient may be written

$$R_{m+1} = \frac{r_{m+1} + R_m \exp(-2i\delta_m)}{1 + r_{m+1} R_m \exp(-2i\delta_m)} \qquad \ldots\ldots(44)$$

or

$$R_{m+1} = \tanh \tfrac{1}{2}(A_m + B_m) \qquad \ldots\ldots(45)$$

where we write

$$A_m = 2 \operatorname{arc\,tanh} r_{m+1} \qquad \ldots\ldots(46)$$

$$B_m = 2 \operatorname{arc\,tanh} [R_m \exp(-2i\delta_m)]. \qquad \ldots\ldots(47)$$

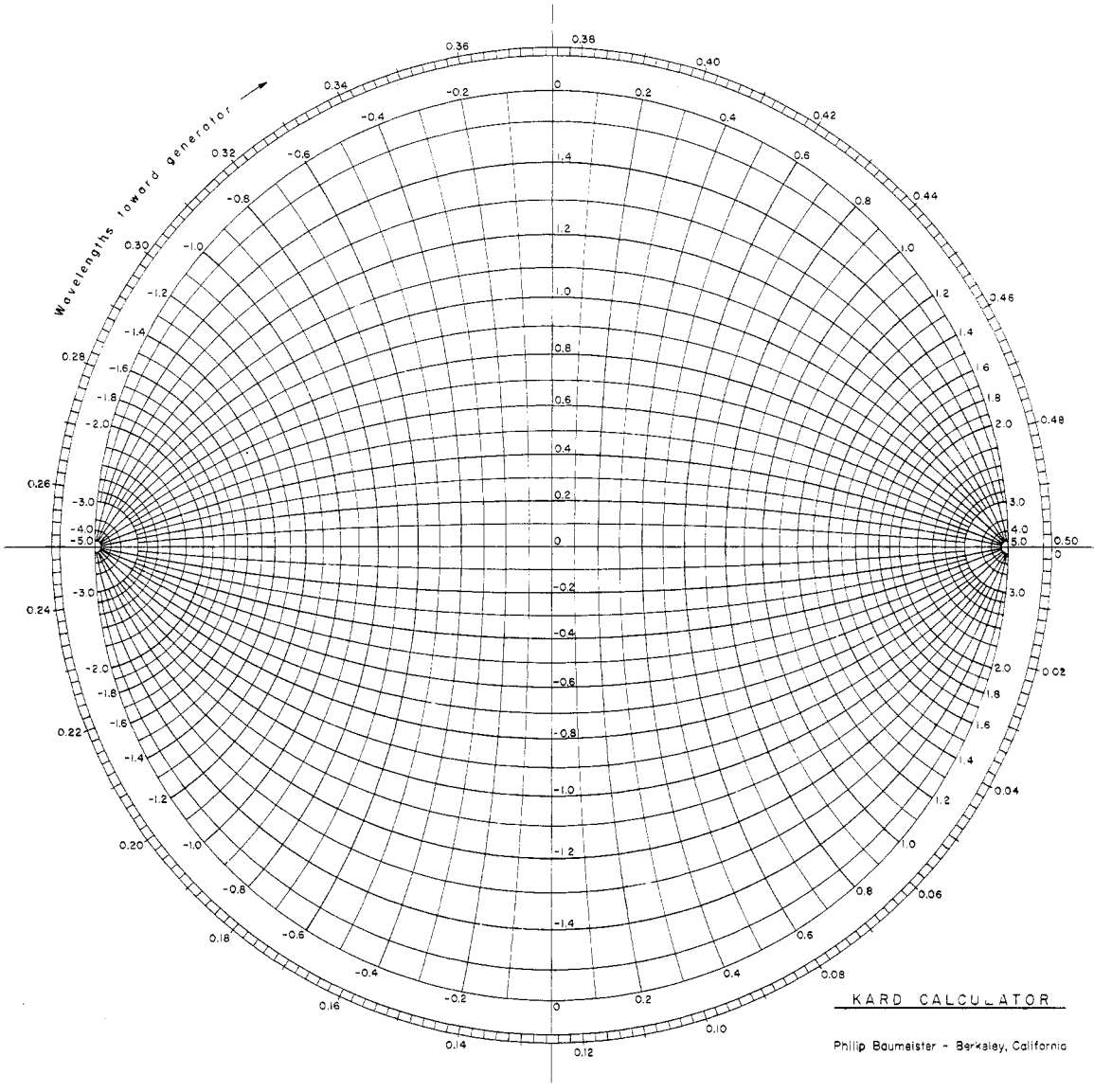

Figure 6. Kard's calculator.

The Kard calculator† (figure 6) is a mapping of the conformal transformation $z = \tanh \frac{1}{2}w$ which thus enables A_m, B_m and R_{m+1} to be determined from given values r_{m+1} and $R_m \exp(-2i\delta_m)$. If all the layers are non-absorbing then the values of A_m [equation (46)] are all real. For normal incidence these simply take the form

$$A_m = 2 \operatorname{arc\,tanh}\left(\frac{n_{m+1}-n_m}{n_{m+1}+n_m}\right) = \ln\left(\frac{n_m}{n_{m+1}}\right). \qquad \ldots\ldots(48)$$

4.4. *General Features governing the Design of Multilayer Systems*

The use of the digital computer for solving multilayer problems has been mentioned above (§ 4.2). Such methods have reached an impressive degree of sophistication in which the computer, on being presented with a trial multilayer system and with data for the desired reflectance or transmittance characteristic, refines the parameters of the multilayer in order to achieve the desired result. It is, however, necessary that the trial system with which the computer is provided shall possess characteristics fairly close to the ideal. For this reason, methods which enable the general features of a multilayer system to be predicted may well serve a useful purpose.

Epstein (1952) has examined the properties of some symmetrical systems of films, making use of the general results of the treatment of Herpin (1947) that a symmetrical system may be reduced to a single film with a certain equivalent index and thickness. These quantities may be readily obtained from the parameters of the system : Epstein gives results for three-layer systems. The transmission characteristics of the system are found to be divided between pass bands, in which the equivalent index is real, and high-reflectance (' stop ') bands, for which the equivalent index is imaginary. In the pass-band the equivalent thickness is approximately equal to the real thickness. The behaviour of the system in these bands is therefore easily visualized in terms of the (known) properties of a single layer.

In an alternative approach Smith (1958) shows that a multilayer system may be reduced to two interfaces. This representation is not confined to symmetrical systems. (The reflection properties of the representative interfaces may be such that they would not be shown by a single equivalent film : this is of no consequence since the behaviour of the system is deduced from the reflectance characteristics of the interfaces and not from equivalent film constants.) The transmission characteristic of a system with two interfaces is easily represented in terms of the Airy sum, and the dependence of such characteristics on the reflectances at the two interfaces is easily visualized. Successive application of this approach enables the properties of various more complex systems to be qualitatively deduced. Thus the properties of systems of mixed quarter- and half-wave layers are readily predicted. In application of the method to these systems, the conditions necessary for narrow-band, wide-band and low-pass (in frequency) filters are readily obtained. The properties of some of these systems are discussed in § 8.

† The copy of the Kard calculator is reproduced by kind permission of Dr. P. W. Baumeister of Rochester, N.Y.

§ 5. Measurement of Film Thickness and Optical Constants

5.1. *General*

The method used for the determination of the thickness of a film depends on a large number of factors. The film may be transparent or absorbing, as may also be the substrate. The edge of the film may be accessible, enabling interference step methods to be used ; in this case, however, care is needed if part of the film lies below the surrounding surface as in the case of a metallic oxide. The choice of method depends on the order of the thickness involved : we shall deal with methods suitable for films up to thickness of the order of microns.

It must be mentioned that in certain cases the film thickness—or, rather, the quantity yielded by the methods of measurement given below—may not be a very well-defined physical quantity. In the case of aggregated films, in which the diameters of aggregates may exceed the mean thickness $\bar{t}$ (defined, for example, as $A^{-1}\Sigma t\,\delta A$ where A is the area), the mass per unit area is perhaps the only useful parameter. The mass per unit area of films of the order of a centimetre square may be determined directly by microbalance (Clegg and Crook 1952, Bradley 1953), with which films of down to about 1 mμ may be handled. Microchemical techniques exist for the estimation of microgramme quantities of many elements (Sandell 1944, Johnson 1955) which in favourable cases enable the mass of 1 cm$^2 \times 10$ mμ films to be determined to better than about 0·5% (Heavens 1959). These methods have the drawback that the film is destroyed in the measurement process. Direct thickness measurement using the ' Talysurf ' instrument enables measurements of the order of 20 mμ to be made within ± 2 mμ ; this method is suitable for hard, coherent films (soft films may be damaged by the stylus). Electrical resistance measurements are in principle sensitive enough for thickness measurements down to a few tenths of a millimicron, but the resistivity of such films is generally so critically dependent on the conditions of preparation, nature of substrate, age, etc., that such methods can be used only with great circumspection. The experiments of Alderson and Ashworth (1957) show, however, that reproducible results may be obtained with nickel–chromium films of thicknesses up to a few tens of millimicrons provided the conditions of preparation are adequately standardized. With the many other electrical measurements which depend on film thickness—electrolytic methods, work function measurements, capacity measurements—the dependence of the electrical properties on thickness needs first to be determined ; this may be a major project. More direct methods are to be preferred.

5.2. *Optical Methods for Measurements of the Thickness and Optical Constants of Films*

Several methods are available for determining thickness and/or optical constants of films, the general requirement being that the films have a smooth surface and lie on a smooth substrate. The methods may be classified roughly as follows.

Interferometric methods. Certain of these methods utilizing fringe displacements, give the film thickness only, independently of the optical constants of film and substrate. Others entail the location of the wavelengths of interference maxima and minima ; these require a knowledge of the optical properties of the substrate.

Photometric methods. Measurements of the reflectance at each side of a film on a transparent substrate can yield the thickness of the film and the optical constants simultaneously, albeit with considerable labour.

Polarized light methods. A study of the state of polarization of light reflected from a film-covered surface may yield information on the film thickness and optical constants. The quantities generally determined are (i) the difference Δ in the phase change on reflection for the two components of polarization and (ii) the ratio of the amplitudes of the two reflected components. In the case of films on transparent substrates, measurements of reflectance and transmittance may be combined with phase change measurements.

5.2.1. *Interferometric, fringe-displacement, methods.*

One of the simplest methods of measuring film thickness is that using multiple-beam interference fringes (Tolansky 1948). The edge of the film is coated with an opaque silver film and measurements are made on the shift in the reflection fringes (Fizeau fringes) observed with a monochromatic source. Interference takes place between the silvered surface and a heavily silvered reference flat. If the order of interference can be made very low, the fringes are extremely fine and an accuracy in a typical case of ± 1 mμ can be obtained.

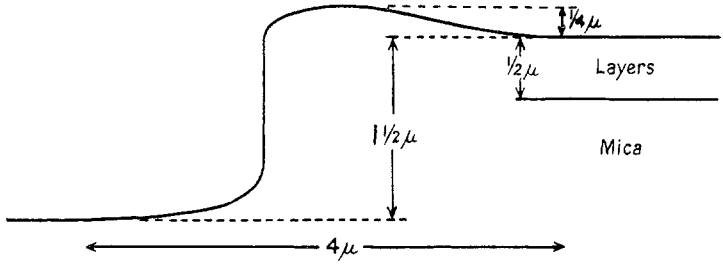

Figure 7. Distortion at edge of multilayer reflecting stack.

It has been established (Heavens 1951, Weaver and Benjamin 1956) that, provided an opaque reflecting layer is used and there is no chemical or other deterioration of the surfaces, the method yields the true thickness of the underlying film. The thickness of the reflecting layer is unimportant, so long as it is opaque : accurate contouring is reported for thicknesses of a silver coating up to 5 μ (Tolansky 1951). The use of high-reflecting multilayers for this purpose, in place of silver films, has been studied (Belk, Tolansky and Turnbull 1954) : the lower absorption attainable in a dielectric multilayer is an advantage. Comparison of thickness measurements using silver and multilayer reflectors shows close agreement. There is a slight tendency to distortion (figure 7) of the contouring of the multilayer at the extreme edge of the step.

Fringes which are inherently sharper than Fizeau fringes and which are formed by illuminating a parallel-sided interferometer with white light and then dispersing the reflected (or transmitted) light may be used for thickness measurement (fringes of equal chromatic order). Although in principle a greater accuracy is attainable with these latter fringes than with Fizeau, it is necessary to apply corrections before an accurate result is obtained. Since white light is used, and measurements

are made on fringes of different wavelengths, correction for the phase change on reflection at the silver (or multilayer) surfaces must be applied. In view of the variation between different observers' results for measurement of phase changes on evaporated metal films, arising from the dependence of this quantity on the precise conditions of preparation of the film, this correction cannot easily be applied. Experiments by Scott, McLaughlan and Sennett (1950) suggest that phase change effects are negligible: the step heights deduced from fringes of orders 1 to 30 are found to be the same even if no phase change effect is assumed. This is, in fact, slightly strange since if the phase change correction is calculated using published values of optical constants, there should be a most marked influence over the range of wavelengths used. In a similar arrangement, systematic errors in thickness measurements are reported by Koehler (1953). When multilayers are used as reflectors the effect of phase changes on reflection is much larger than with a metal reflector and must be allowed for. The procedure to be followed is given by Koehler (1955). The phase change on reflection is not required explicitly but may be eliminated by suitable treatment of the data. In fact, Koehler additionally calculated the effect of phase changes from the known constants of the multilayers used, by means of equation (41), and obtained good agreement over the range of ± 100 mμ from the wavelength at which the peak multilayer reflectance occurs. In measurements of a step height using five fringes over the range 460 to 560 mμ, the result obtained was $63{\cdot}0 \pm 0{\cdot}2$ mμ. The effect of phase changes in white light interferometry has also been studied by Schulz and Scheibner (1950), by Schulz (1951) for silver, and by Rank and Bennett (1955) for multilayers and aluminium films.

The great advantage of multiple-beam methods such as those described above is that, if a metal reflector layer is used on the film to be measured, the measurements made are entirely independent of the optical properties of film and substrate. Either may be transparent or absorbing. In principle, the phase properties of a multilayer will depend on the optical constants of the substrate. For a multilayer with many layers on a transparent substrate, the dependence on substrate properties will be slight.

The use of Fabry–Perot and Michelson interferometers for film thickness measurement of transparent films have been described by Schulz (1950) and Fochs (1950). In Schulz's method, the film is deposited over part of an optical flat which is then heavily silvered and used as one mirror of a Fabry–Perot interferometer, illuminated with sodium light. There are then two successive positions of the mirror, separated by a distance M mm, in which the Fabry–Perot fringes appear as shown in figure 8. The film thickness may be determined from M; the wavelength difference between the sodium lines is used as an internal standard. The film thickness t in mμ is given by $t = 507M$. The setting of figure 8 can be made to within a tenth of a fringe, corresponding to $\pm 1{\cdot}5$ mμ in film thickness. The possible effect of a different substrate on the phase change on reflection of the silver film is not discussed although the effect for high-reflecting silver films is probably negligible.

Both film thickness and refractive index of a (non-absorbing) film are obtained by the use of the Michelson interferometer with a white light source. The film is placed so as to intercept part of one of the two beams. Part of one mirror is

covered by an opaque screen (figure 9) so that the fringes seen in the dispersing system from this region (A) arise from multiple reflections in the film. Normal Michelson fringes are seen from region C whilst those from B are displaced on

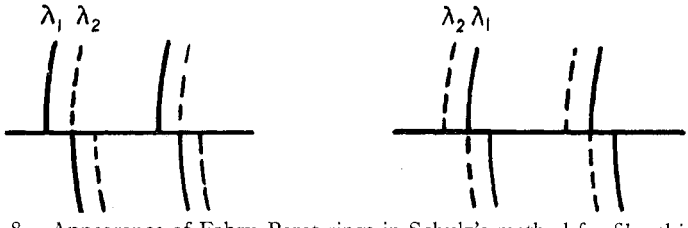

Figure 8. Appearance of Fabry–Perot rings in Schulz's method for film thickness.

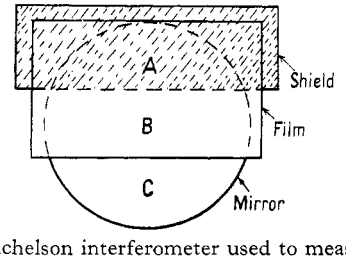

Figure 9. The Michelson interferometer used to measure film thickness.

account of the change in path difference of $2(n-1)\,d$ introduced by the film. When the Michelson mirror separation is equal to $2d$ the fringes from regions A and B are complementary. An accuracy to $\pm 0{\cdot}02\ \mu$ is quoted for a specimen 12 μ thick. The refractive index is determined to $\pm 0{\cdot}003$.

5.2.2. *Photometric methods.*

There are two general methods in this class: the method described by Schopper (1952 b) entails measurement of the amplitude and phase of the light reflected from each side of a film and of the light transmitted by the film, all the measurements being at (or as near as is possible to) normal incidence. Although three measurements should suffice to determine the three unknowns n_1, k_1, d_1, the nature of the equations relating reflectance and transmittance to these quantities is such that n_1, k_1 and d_1 cannot be written explicitly in terms of only three measurables.

Denoting by S_i, ϕ_i the amplitudes and phase changes on reflection in media n_0, n_2 (figure 10), S, ϕ the amplitude and phase change on transmission, and writing

$$\epsilon_2 = \phi_2 - \pi + \frac{4\pi n_2 d_1}{\lambda} \qquad \ldots\ldots(49)$$

and

$$\epsilon = \phi + \frac{2\pi n_2 d_1}{\lambda}, \qquad \ldots\ldots(50)$$

the index $n_1 - ik_1$ of the film is obtained in terms of the observables as

$$(n_1 - ik_1)^2 = n_0 \frac{n_0^2 S_2 \exp(i\epsilon_2)\,[1 + S_0 \exp(i\phi_0)]^2 - n_2 S^2 \exp(2i\epsilon)\,\{n_2 - n_0[1 + S_0 \exp(i\phi_0)]\}}{n_0 S_2 \exp(i\epsilon_2)\,[1 - S_0 \exp(i\phi_0)]^2 + S^2 \exp(2i\epsilon)\,\{n_0 - n_2[1 - S_0 \exp(i\phi_0)]\}} \qquad \ldots\ldots(51)$$

from which n_1 and k_1 are determined. The film thickness is then obtained from

$$\exp\left(\frac{4\pi i n_2 d_1}{\lambda}\right) = \frac{-S_2 n_0[(n_1-ik_1)^2-n_2^2]\exp(i\epsilon_2)}{(n_1-ik_1)^2\{n_0-n_2[1-S_0\exp(i\phi_0)]\}+n_2 n_0\{n_2-n_0[1+S_0\exp(i\phi_0)]\}}. \quad \ldots\ldots(52)$$

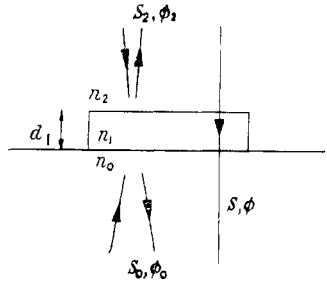

Figure 10.

The quantities ϵ, ϵ_2 introduced in (49) and (50) are seen to be the differences in the phase changes on reflection and transmission at the filmed and uncoated parts of the substrate. These are more readily measurable than the ϕ values.

This method possesses the advantage that (i) the thickness and optical constants are determined simultaneously and (ii) monochromatic light is used so that no errors from neglected dispersion effects arise. The disadvantage is that rather elaborate experimental arrangements are needed in order to make the (absolute) reflectance, transmittance and phase change measurements with sufficient accuracy. The accuracy of measurements made on films of up to 200 mμ thickness was estimated as to ± 3 mμ on thickness and to $\pm 0{\cdot}03$ on the optical constants.

Measurements of phase changes are avoided in the method introduced by Malé (1952), developed from an earlier method by Murmann (1933, 1936), in which the thickness and optical constants are determined from the measured reflectances and transmittance. Since it is impossible to express n_1, k_1 and d_1 explicitly in terms of the measured quantities the following indirect method is used. Sets of curves are first prepared giving **R**, **R′** (reflectances at either side of the film) and **T** as functions of $\delta \equiv 4\pi n_1 d_1/\lambda$ for a (two-dimensional) range of values of n_1 and k_1. These may be calculated from equations (13) and (14) by inserting $n_1 - ik_1$ in the expressions for the Fresnel coefficients. In closed form, for a film on a non-absorbing substrate of index n_0, the expressions for **R**, **R′** and **T** are

$$\mathbf{R} = \frac{(g_2^2+h_2^2)\exp(2\alpha_1)+(g_1^2+h_1^2)\exp(-2\alpha_1)+2(g_1g_2+h_1h_2)\cos 2\gamma_1+2(g_2h_1-g_1h_2)\sin 2\gamma_1}{\exp(2\alpha_1)+(g_1^2+h_1^2)(g_2^2+h_2^2)\exp(-2\alpha_1)+2(g_1g_2-h_1h_2)\cos 2\gamma_1+2(g_2h_1+g_1h_2)\sin 2\gamma_1} \quad \ldots\ldots(53)$$

$$\mathbf{T} = \frac{n_0}{n_2}\,\frac{[(1+g_1)^2+h_1^2][(1+g_2)^2+h_2^2]}{\exp(2\alpha_1)+(g_1^2+h_1^2)(g_2^2+h_2^2)\exp(-2\alpha_1)+2(g_1g_2-h_1h_2)\cos 2\gamma_1+2(g_1h_2+g_2h_1)\sin 2\gamma_1} \quad \ldots\ldots(54)$$

where
$$\alpha_1 = 2\pi k_1 d_1/\lambda, \qquad \gamma_1 = 2\pi n_1 d_1/\lambda,$$
$$g_1 = \frac{n_1^2 - n_0^2 + k_1^2}{(n_0+n_1)^2 + k_1^2}, \qquad h_1 = \frac{-2n_0 k_1}{(n_0+n_1)^2 + k_1^2},$$
$$g_2 = \frac{n_2^2 - n_1^2 - k_1^2}{(n_2+n_1)^2 + k_1^2}, \qquad h_2 = \frac{2n_2 k_1}{(n_2+n_1)^2 + k_1^2}.$$

R′ is obtained by interchanging in the numerator of equation (53) the coefficients of $\exp(2\alpha_1)$ and $\exp(-2\alpha_1)$. The denominator is unchanged. Alternatively graphical methods such as those of Malé (1950) or of Kard given above may be used. From each of the curves so prepared, values of **R**, **R**′ and δ, corresponding to the experimentally observed value of **T**, may be obtained for various values of n_1 and k_1. Curves are then plotted of **R** against k_1 for each value of n_1 from which are read off pairs of values of (n_1, k_1) corresponding to the observed value of **R**. These points are plotted on a curve of k_1 against n_1. The whole procedure is then repeated for **R**′ in place of **R** and a second curve of k_1 against n_1 plotted. The required n_1 and k_1 are given by the intersection of the two curves. With n_1 and k_1 known, d_1 is obtained by plotting δ against n_1 for various k_1 and deducing the δ corresponding to the values of n_1, k_1 by interpolation.

This method has been extensively used by Malé and his collaborators in studies of the properties of metal films formed by thermal evaporation. The results of these experiments are discussed in § 6.1.

5.2.3. *Polarization methods.*

For a considerable time use has been made of the fact that measurements of the state of polarization of light beams may be made with high accuracy. Light reflected from a surface is generally elliptically polarized : by compensating the phase difference Δ between the p- and s-reflected components, plane polarized light is produced. The angle ψ ($= \arctan R_p/R_s$) between the plane of the electric vector and the plane of incidence is accurately measurable. The values of Δ and ψ depend sensitively on the presence of a film on the surface. In contrast to the interferometric methods given in § 5.2.1 however, the values of the optical constants of the substrate must be known. These are determined by standard polarimetric procedures (see, for example, Bor and Chapman 1949, Winterbottom 1946) on an uncoated part of the substrate. Alternatively, where substrates may be prepared bearing stepped films, the optical constants of the underlying metal may be eliminated. This method is discussed in § 5.2.4 below.

Transparent films.

(i) *Drude's approximation.* As early as 1889, Drude gave expressions, valid for films of thickness $d \ll \lambda$, enabling the thickness and refractive index to be determined from the measured differences in Δ and ψ for coated and uncoated parts of the substrate. The validity of these equations has been examined by Rothen and Hanson (1949) for films of barium stearate on stainless steel, close agreement being obtained for thicknesses up to 25 mμ.

(ii) *Vašíček's method.* If the Drude method is extended to deal with films of any thickness, it is no longer possible to deduce the values of index and thickness

directly from the equations. Vašíček (1947) has dealt with the problem of a transparent film on a glass substrate, giving a procedure whereby the values of n and d can be obtained. With the notation of § 3.2, the values of Δ and ψ are readily seen to be given by

$$\tan\Delta = (AB' + AB')/(AA' - BB') \qquad \ldots\ldots(55)$$

where

$$A = r_{1p}(1 + r_{2p}^2) + r_{2p}(1 + r_{1p}^2)\cos 2\delta_1$$

$$A' = r_{1s}(1 + r_{2s}^2) + r_{2s}(1 + r_{1s}^2)\cos 2\delta_1$$

$$B = -r_{2p}(1 - r_{1p}^2)\sin 2\delta_1$$

$$B' = r_{2s}(1 - r_{1s}^2)\sin 2\delta_1$$

and

$$\tan^2\psi = \frac{(r_{1p}^2 + r_{2p}^2 + 2r_{1p}r_{2p}\cos 2\delta_1)(1 + r_{1s}^2 r_{2s}^2 + 2r_{1s}r_{2s}\cos 2\delta_1)}{(1 + r_{1p}^2 r_{2p}^2 + 2r_{1p}r_{2p}\cos 2\delta_1)(r_{1s}^2 + r_{2s}^2 + 2r_{1s}r_{2s}\cos 2\delta_1)}. \qquad \ldots\ldots(55a)$$

In Vašíček's experimental arrangement plane polarized light is incident with its plane of polarization inclined at 45° to the plane of incidence. The ellipticity of the reflected light is measured using a Senarmont compensator and Nakamura double plate (Vašíček 1940).

Equations (55) and (55a) cannot be solved directly for n_1 and d_1 but are dealt with by successive approximation. Vašíček gives a table of values of ψ and Δ for films of thickness up to 1–1·5 μ and for refractive indices 1·2 to 2·75 for a substrate of index 1·5163 and for $\lambda = 589$ mμ. Vašíček's claim that the method is sufficiently sensitive to detect films 1 mμ thick has been challenged by Mattuck (1956). It would appear that Vašíček's claim implies a precision of 0·5′ in the determination of Δ, ψ. In Mattuck's experimental arrangement, a precision of $\pm 2{\cdot}5'$, corresponding to a limiting film thickness of 5 mμ, was recorded.

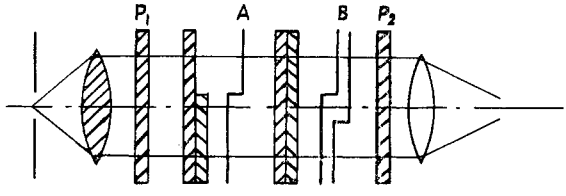

Figure 11. Thickness measurement using the Françon eyepiece (van Heel).

(iii) *Use of the Savart plate.* An accuracy to $\pm\lambda/200$ can be attained in the measurement of the refractive index and thickness of a transparent film on a transparent substrate by the use of the eyepiece devised by Françon (1952, 1953, 1954). Plane polarized light from the polarizer P_1 (figure 11) emerges from the film and substrate with the wave front deformed as shown at A. The Savart plate in the eyepiece produces two mutually perpendicularly polarized component wave fronts which are displaced laterally with respect to each other (B). Viewed through the analyser P_2 the field of view will then in general show three different intensities, if monochromatic light is used, or three different colours, if white light is used. The use of monochromatic light is to be preferred unless the effects of dispersion can be adequately allowed for. Various experimental arrangements are discussed by van Heel and Walther (1958) for determining the phase difference introduced by

the film and the transmittance of the film from which, with the help of equation (14), the film thickness and refractive index are determined. Since normal incidence on the film is used and since no silvering is involved, the method is particularly suitable for, for instance, the continuous monitoring of the thickness of a film during deposition.

(iv) *Zernike–Dyson method.* This arrangement, in which high sensitivity is achieved by the use of a half-shade system, is one of the most sensitive to date for the measurement of the metrical thickness of a film. The edge of the film must be accessible and the surface is aluminized. Light from a slit is projected, via a Wollaston prism, on to the film surface, producing two images at the surface which are perpendicularly polarized. On re-passing the Wollaston prism the images are combined and the final image is examined through a polarizer and half-shade system. The dividing edge of the latter lies across the slit image. Settings for the equality of brightness are made (i) with the two slit images astride the film edge and (ii) with both images on one side of the film edge. Special arrangements are necessary to ensure that the setting adjustments do not alter the conditions of polarization. A repeatability to $\pm 0{\cdot}1$ mμ is obtained (Dyson 1958) in a system in which no serious precautions were taken against mechanical or thermal drifts.

Absorbing films.

The method due to Vašíček given above may be used to deal with absorbing films if the thickness is determined independently. Tables are given (Vašíček 1951) enabling the optical constants to be determined from the observations for the following ranges :

Thickness	to 100 mμ by 10 mμ
n	1·00 to 2·75 by 0·25,
k	0 to 1·0 by 0·2

Equations enabling the optical constants and film thickness to be deduced from measurements of the ellipticity of light transmitted by, and reflected from, each side of a film have been given by Försterling (1937). No approximations are involved. When this method was applied, complex values were obtained for the film thickness. This is likely to be a manifestation of anisotropy in the film and suggests that this method may be unduly sensitive to a departure from isotropy or homogeneity of the film. Since anisotropy in films generally takes the form of an optic axis normal to the substrate, methods involving only normal incidence measurements are to be preferred.

For dealing with absorbing films of such thickness and absorption that multiple reflections in the film may be neglected, Leberknight and Lustman (1939) use approximations which are found to be valid, for several metal oxides, for thicknesses up to several tens of millimicrons.

5.2.4. *Methods employing stepped reflectors.*

These methods make use of the fact that monomolecular layers of certain fatty acids and their salts may be easily picked up from a water surface. Multiple layers of such films are found to be stable and to behave accurately reproducibly in respect of their physical properties. Barium stearate has been used extensively.

Its properties have been very thoroughly investigated by Blodgett and Langmuir (1937). Such films may be built up to any number of layers. Their optical properties were fully investigated, using polarimetric and Brewster angle techniques, from which the thickness per film was deduced as 2·44 mμ.† The films are found to be uniaxial, with optic axis normal to the plane of the film, and with refractive indices $n_1 = 1{\cdot}491$ (ordinary) and $n_3 = 1{\cdot}551$ (extraordinary) for $\lambda = 589$ mμ.

Use is made of such films in an ingenious arrangement by Rothen (1945) for the determination of the optical thickness of films of thicknesses down to a few tenths of a millimicron. Different numbers of BaSt layers are picked up on two halves of a polished chromium slide. The slide is illuminated with plane polarized light which is reflected through a mica $\lambda/4$ plate so arranged that elliptically polarized light (of very small ellipticity) from one half of the field is left-handed and that of the other half right-handed. An analyser is adjusted for equality of brightness in the two fields. When a further film is deposited over the whole slide the brightnesses of the two fields become unequal in the manner obtaining in the usual half-shade system. Measured rotation of the analyser restores the uniformity of brightness and the amount of rotation yields the film (optical) thickness. When a BaSt layer was used as the added film, the rotation of the analyser was 3·2°. Since a rotation of 0·02° is detectable and since the thickness of one BaSt layer is 2·4 mμ the noise level of the measurement is of the order of 0·03 mμ. It must be stressed that this method yields the *optical* thickness and that the refractive index must be determined independently if the metrical thickness is required.

It is suggested by Hartman (1954) that the above procedure is liable to be in error if the index of the added film differs from that of the substrate. If the objection is valid the method becomes severely limited in scope. The grounds for the objection are not, however, made clear and no substantiation is given. The method proposed by Hartman in the same paper is the subject of some criticism by Mattuck (1956), who claims that the approximations used are not valid for films thicker than about 1 mμ.

For the study of films of the BaSt type, which may be stacked on a substrate in known numbers, Hartman *et al.* (1954) employ an interferometric method in which white light, plane polarized with the electric vector perpendicular to the plane of incidence, is incident on the surface bearing a suitable number of films (21 for BaSt). The reflected light is passed through an analyser set at 90° to the plane of incidence and is passed to a dispersing system. The s-component of the amplitude reflectance of the filmed surface is given by

$$R_s = \frac{r_{1s} + r_{2s}\exp(-2i\delta_1)}{1 + r_{1s}r_{2s}\exp(-2i\delta_1)} \qquad \ldots\ldots(56)$$

and will be a minimum for some values $2\delta_1 = C$, say, and for other values $2\delta_m$ such that

$$2\delta_m = C + 2m\pi \qquad \ldots\ldots(57)$$

where m is an integer. (The result holds only if dispersion of the optical constants of film and substrate are neglected. These assumptions are reasonably justified for BaSt on chromium for visible wavelengths.)

† Subsequent measurements give the slightly lower value of 2·28 mμ.

If d_0 is the thickness of one BaSt double layer and N is the number of double layers on the slide, then for an angle of incidence ϕ :

$$m = \frac{2Nd_0(n_1^2 - \sin^2\phi)^{1/2}}{\lambda} - \frac{C}{2\pi} \qquad \ldots\ldots(58)$$

where n_1 is the index of the film. A plot of m, the order of the dark fringe observed in the spectrograph, against N/λ yields a straight line of slope $b_1 = 2d_0(n_1^2 - \sin^2\phi)^{1/2}$. From this relation,

$$\sin^2\phi = -\frac{b_1^2}{4d_0^2} + n_1^2. \qquad \ldots\ldots(59)$$

Measurements are made at several angles of incidence (ranging from 70° to 85°) and the value of d_0 obtained from a plot of $\sin^2\phi$ against b_1^2. The refractive index is obtained from the slope of the line. From these experiments, the values of d_0 and n_1 (which corresponds to the ordinary index) are $d_0 = 4{\cdot}57 \pm 0{\cdot}07$ mμ, $n = 1{\cdot}508 \pm 0{\cdot}013$.

This method has been further developed by Mattuck, Petti and Bateman (1956). A stepped interference reflector consisting of two BaSt steps (of 20 and 40 double layers) is used. Fringes are formed in the focal plane of a dispersing system as in the Hartman method. Measurements are made of the displacements of fringes from both halves of the field when an unknown layer is deposited over the whole of the slide carrying the stepped reflector. For refractive indices in the range 1·1 to 2·0 and for thicknesses from 2 mμ to 25 mμ a sensitivity to 1% in refractive index and 4% in thickness is claimed. It is suggested that errors arising from neglect of birefringence in the BaSt films and of dispersion may be negligible. The values obtained for the refractive indices of several evaporated films (Mattuck, Petti and Bateman 1956) were found to agree within the experimental error with those obtained by the Abelès method (see §5.2.6 below). In general, the accuracy of the Abelès method is higher ; this method does not, however, give the film thickness.

5.2.5. *Separate measurement of n and k.*

Whilst the simultaneous measurement of n and k on one film eliminates any variation between different samples, it is a fact that n and k can be more accurately determined by separate experiments. Thus k may be accurately determined by transmission measurements, or by measurements of the phase change on reflection at a surface. With the value of k known, n is accurately obtained from measurements of the reflectance at the surface. These methods have been developed by Schulz and Tangherlini (1954) in experimental studies relating to the Drude free electron theory of metals. Measurements were made on metal films formed by thermal evaporation and annealed. The criterion for homogeneity adopted is the relation between the reflectances of the p- and s-components predicted by electromagnetic theory. For reflection at the interface between homogeneous media at an angle of incidence of 45°, $\mathbf{R}_s^2 = \mathbf{R}_p$. This relation was found to be satisfied by suitably annealed films of silver, aluminium and copper.

Calculation of the transmission of films of various thickness yields curves such as those of figure 12. The departure from linearity at small thicknesses arises

from the effect of reflections at the interfaces. When the thickness is sufficiently large the effect of multiple reflections in the film becomes negligible : under this condition the transmittance is given by

$$\mathbf{T} = \frac{16n_0 n_2(n_1^2+k_1^2)^2}{[(n_1+n_2)^2+k_1^2]\,[(n_0+n_1)^2+k_1^2]} \exp\left(-\frac{4\pi k_1 d_1}{\lambda}\right). \quad \ldots\ldots(60)$$

From this equation we see that k_1 can be obtained from the slope of the curve of ln $\mathbf{T}$ against d_1. (Although in principle the intercept of this curve could yield n_1, using the k_1 value from the slope, Schulz suggests that the k value in the intercept term is likely to differ from that in the exponential term, on account of surface defects.)

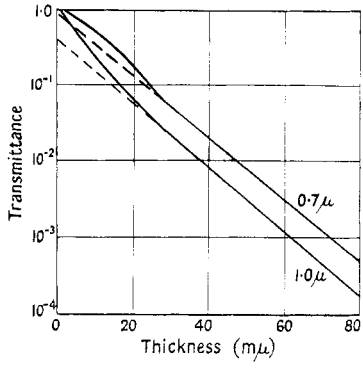

Figure 12. Calculated transmittance–thickness curves for silver films. The measured optical constants at $\lambda = 0{\cdot}7\ \mu$ and $\lambda = 1{\cdot}0\ \mu$ are used in the calculation.

An interesting alternative method for k is to make an interference filter and to deduce the value of the phase change α on reflection at the metal–dielectric interface from the effect of such phase change on the wavelengths of the transmission maxima, when white light is incident on the filter. k is then calculated from the equation

$$\tan\alpha = \frac{2k_1 n_0}{n_1^2+k_1^2-n_0^2} \quad \ldots\ldots(61)$$

where n_0 is the refractive index of the dielectric layer. The method requires (i) that the dispersion of the dielectric is known and (ii) that the metal film is thick enough for equation (61) (which holds for reflection at a bulk surface) to be valid. Furthermore, if the wavelengths of the transmission maxima are to be accurately measurable, the fringes must be sharp and hence the reflectivity of the metal films used must be high. This would seem to limit the method to metals with a large reflectivity and small ratio of absorption to transmission.

Measurement of the value of n is effected by measuring the reflectance at 45° of a thick (> opaque) film of the metal. In order to avoid the danger of atmospheric contamination, the reflection at the substrate side is measured (figure 13). A simple approximation method enables n to be obtained, using the value of k obtained, for example, in the transmission experiment reported above.

Since these methods were evolved with a view to studying the values of n and k, the film arrangements have been designed to suit the experiments rather than vice

versa. It is likely that the values of n and k obtained in these experiments are the most reliable to date.

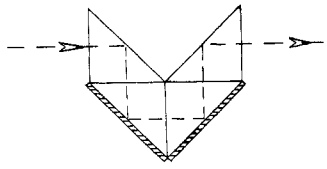

Figure 13. Arrangement for measuring the reflectance, at 45°, at the film–substrate interface.

5.2.6. *Brewster angle method for refractive index.*

The refractive index alone of a transparent film is conveniently measured by the method introduced by Abelès (1950). A collimated beam of plane polarized light ($E \parallel$ plane of incidence) is incident on a surface partly covered by the film under investigation. The angle of incidence ϕ_B for which the reflectance of film and substrate are equal is determined. If the light is incident in air, then the index n of the film is simply given by

$$n = \tan \phi_B. \qquad \ldots\ldots(62)$$

This result is independent of the thickness of the film and of the optical constants of the substrate. The *sensitivity* of the method does, however, depend on these quantities. For measurements on a transparent substrate, provided that the index of the film lies within $\pm 0{\cdot}3$ of that of the substrate, an accuracy to $\pm 0{\cdot}002$ is attainable in films of suitable thickness. Since monochromatic light is used, no errors from dispersion effects arise. A particularly convenient experimental arrangement for this method is described by Traub and Osterberg (1957). The method has been applied to the study of oxide films on metals : for this measurement, a photometric detector may be needed in order to discriminate the small change in brightness around the Brewster angle ϕ_B. A suitable scanning method, in which a half-coated specimen is rotated rapidly and reflected light collected by a photomultiplier has been described by Heavens and Kelly (1959). For 50 mμ films of tantalum oxide on tantalum, an accuracy to $\pm 0{\cdot}003$ was obtained.

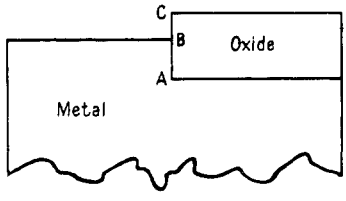

Figure 14. Schematic diagram of partly oxidized metal surface.

Measurements of the reflectance of the filmed surface in the neighbourhood of the Brewster angle may be used to check whether the film is homogeneous. The Brewster angle measurement yields an index value which may be combined with a thickness measurement using multiple-beam Fizeau fringes to enable the reflectance (on the assumption of uniformity) to be calculated using equation (13). For tantalum oxide films, significant differences between experimental and calculated values indicate a slight lack of homogeneity in the film (Heavens and

Kelly 1958). In measuring the thickness of metallic oxide films by Fizeau fringes it is necessary to measure both the steps AB and BC shown in figure 14 and to note that the fringe displacement corresponding to the step AB depends on the refractive index of the film (Kelly 1958 a).

5.2.7. *Spectrophotometric methods of thickness and index determinations.*

If white light is reflected at a film-covered surface and the reflected light dispersed, maxima and minima are observed at various wavelengths in the spectrum. The positions of such turning values are determined by the thickness and refractive index of the overlying film, although not in as simple a way as has cheerfully been supposed by some workers. The effective optical path of light in the film is made up of the optical thickness of the film together with the path equivalent of the phase change on reflection at the oxide–metal surface. This is a function of the optical constants of the film and substrate. Since all these quantities are wavelength dependent, the derivation of thickness and index from the wavelengths at turning points is a matter of some difficulty. Furthermore, the phase change on reflection depends on the direction of the plane of polarization. In studies of the oxidation of uranium, Charlesby and Polling (1955) used unpolarized light at non-normal incidence and ignored the change of phase shift with wavelength : these results must therefore be considered as very approximate. (The theory at the beginning of their paper is incorrect.) In experiments on anodic tantalum oxide, phase effects are correctly allowed for by Young (1958) : in these experiments, the refractive index was determined independently by the immersion method. The films were assumed to be homogeneous.

The magnitude of the error involved by neglect of the phase change on reflection has been estimated by Winterbottom (1946) for films on iron, copper and aluminium. The path equivalent of the phase changes are :

Fe_2O_3 on Fe : 15 mμ
Cu_2O on Cu : 22 mμ
Al_2O_3 on Al : 16 mμ

These values are appropriate to $\lambda = 546$ mμ.

5.3. *Summary of Methods available for Optical Constants and Thickness Determinations*

The choice of method to be used depends so much on the nature of the particular problem that no general rules can be given. The table opposite sets out the general features of the methods described.

§ 6. Results of Measurements of Optical Constants of Films

In this section are reviewed results serving to show the general optical behaviour found in thin films. The volume of such studies in recent years is prodigious ; detailed comment will be restricted to cases which have been reasonably thoroughly investigated. Tables of numerical values of optical constants are given at the end of the section.

Summary of Methods for Thickness and Optical Constant Measurement

Method	Quantities measured	Film		Substrate		Measurement gives			Accuracy of thickness	Remarks
		T	A	T	A	d	n	k		
Multiple-beam Fizeau fringes	Fringe displacement	Yes	Yes	Yes	Yes	Yes	—	—	± 1–$1{\cdot}5$ mμ	—
Multiple-beam Feco fringes	Fringe (wavelength) displacement	Yes	Yes	Yes	Yes	Yes	—	—	$\pm 0{\cdot}5$–1 mμ	Correction for phase changes
Fabry–Perot interferometer	Fringe matching. Mirror separation	Yes	Yes	Yes	Yes	Yes	—	—	$\pm 1{\cdot}5$ mμ	—
Michelson interferometer	Fringe matching	Yes	No	Yes	No	Yes	Yes	—	± 20 mμ	—
Schopper	Amplitudes and phases of 2 reflected and transmitted beams	Yes	Yes	Yes	No	Yes	Yes	Yes	± 3 mμ	Simultaneous n, k, d
Malé	Reflectances and transmittances	Yes	Yes	Yes	No	Yes	Yes	Yes	~ 1 mμ	Simultaneous n, k, d
Drude	Δ, ψ	Yes	No	Yes	Yes	Yes	Yes	—	~ 1 mμ	Valid up to 10–20 mμ
Leberknight and Lustman	Δ, ψ	Yes	Yes	Yes	Yes	Yes	Yes	Yes	—	Indirect. Curve-fitting
Vašíček	Δ, ψ	Yes	No	Yes	No	Yes	Yes	—	± 1–2 mμ	Indirect. Tables given for one glass
Savart plate	Colour or intensity matching. Phase difference	Yes	No	Yes	No	Yes	Yes	—	± 3 mμ	—
Zernike–Dyson	Colour or intensity matching	Yes	Yes	Yes	Yes	Yes	No	No	—	—
Stepped reflector	Phase change or fringe wavelength	Yes	No	Yes	Yes	Yes	Yes	—	$\pm 0{\cdot}1$ mμ or 4%	—
Schulz : k	Transmittance for several thicknesses or phase change from fringe displacement	—	Yes	Yes	No	—	—	Yes	—	Methods used together
Schulz : n	Reflectance	—	Yes	Yes	No	—	Yes	—	—	
Abelès	Brewster angle	Yes	No	Yes	Yes	No	Yes	—	—	Very simple
Spectrophotometric	Wavelength of interference maxima and minima	Yes	(Yes)	Yes	Yes	(Yes)	(Yes)	—	—	Phase changes involved, dispersion troubles.

The optical behaviour of films is by now known to be sensitive to film structure which is in turn influenced by the conditions under which the films are formed. Assessment and comparison of much published work in this field is made difficult by the frequent absence of details of the conditions of preparation. Most of the results reported for films formed by thermal evaporation have been obtained on films produced in demountable vacuum systems at pressures in the region of 10^{-5} mm Hg. At this pressure and at the usual rates of deposition quoted, the relative numbers of depositing atoms and of residual gas atoms striking the substrate are comparable. The rate of deposition is therefore expected to influence the film properties. The ability of the deposited atoms to form into crystals will also depend on the rate of arrival of further atoms, a feature clearly shown by the electron micrographs of Sennett and Scott (1950) of silver films. Films deposited slowly are found to be much more granular than those formed rapidly.

The nature and orientation of deposited films may be influenced by the form of the substrate: under certain conditions epitaxial growth may occur. The temperature of the substrate and the effective temperature at which the film forms—a difficult quantity to measure and one over which much argument rages—also have a marked influence on the nature of the resultant film. In the results discussed below such relevant information will be included where this is available.

6.1. *Metal Films*

For most metal films a marked dependence of the optical constants on film thickness is observed. With increasing film thickness, the value of n—initially much higher than that characteristic of the bulk metal—decreases smoothly, reaching a steady value for thicknesses of the order tens of mμ. The extinction coefficient k starts from a very low value and rises, either monotonically or through a maximum, to a limiting value which may be close to the bulk value. This behaviour is interpreted in terms of the aggregated structure exhibited by the films concerned.

The dependence of optical constants on wavelength does not admit of simple generalization. Increases and decreases, with and without maxima and minima, and which are sharply dependent on film thickness, are observed. The general trend observed can be accounted for in terms of the granular structure of the film.

6.1.1. *Gold films.*

Since gold is a noble metal the properties of gold films may be expected to depend less on, for example, the effects of residual gas in the vacuum chamber and on atmospheric contamination than would those of metals susceptible to oxidation. There is a reasonable measure of agreement between different observers' results—even between those for films obtained by sputtering and by evaporation. A comprehensive bibliography of early work is given by Mayer (1950).

Dependence of optical properties on film thickness. The reflectance and transmittance, phase changes and optical constants of gold films have been studied by Rouard, Malé and Trompette (1953) and by Malé and Rouard (1953). Films of several thicknesses were prepared simultaneously by thermal evaporation through a suitably shaped rotating shield (' Talbot Disc '). It is suggested that this procedure ensures that the structures of the films are rigorously identical

although, since the rates of deposition of the various films are different, this assumption may not be justified. The rates of deposition are not given. The results of reflectance and transmittance measurements are shown in figure 15 for

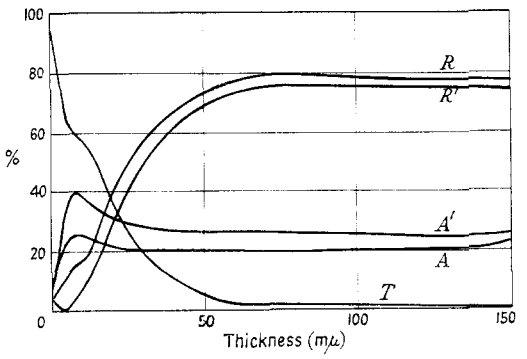

Figure 15. Percentage reflectance, transmittance and absorptance of evaporated gold films, $\lambda = 546$ mμ. (Primes indicate light incident from substrate side.)

light of wavelength 546 mμ. Similar general behaviour is shown for other wavelengths in the visible spectrum except that as shorter wavelengths are approached the limiting reflectances decrease considerably. Although the march of the reflectance–thickness curves is similar in form to that calculated from the bulk

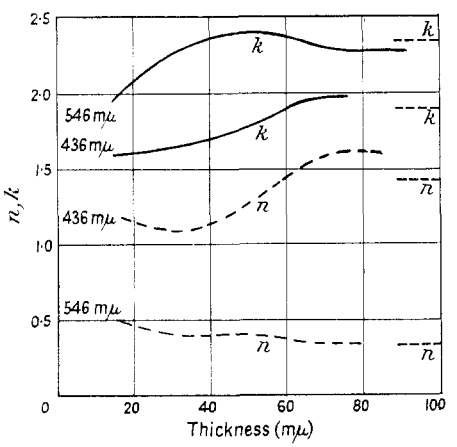

Figure 16. Optical constants of evaporated gold films. Values for annealed, thick films shown at the right-hand side.

values of the optical constants, quantitative agreement is lacking. On the assumption that the films behave as though uniform, the optical constants for the various thicknesses may be calculated. Results obtained from measurements by Malé and Rouard (1953) are shown in figure 16. There is reasonable agreement between the values of n and k for large thicknesses with the values obtained by Schulz (1957) from annealed thick films. These values may be assumed to be characteristic of the bulk metal.

Dependence of optical constants on wavelength. The observed variation with wavelength of n and k for several thicknesses of evaporated gold film is shown in figure 17, together with curves representative of the bulk material. It is found that there are marked differences from bulk behaviour for thicknesses below about 10 mμ. The resistivity of films similarly prepared is found, for thicknesses below about 10 mμ, to be very much higher than that of the bulk metal. This behaviour is consistent with the structure observed by electron microscopy which reveals a collection of isolated, or nearly isolated, aggregates rather than a continuous

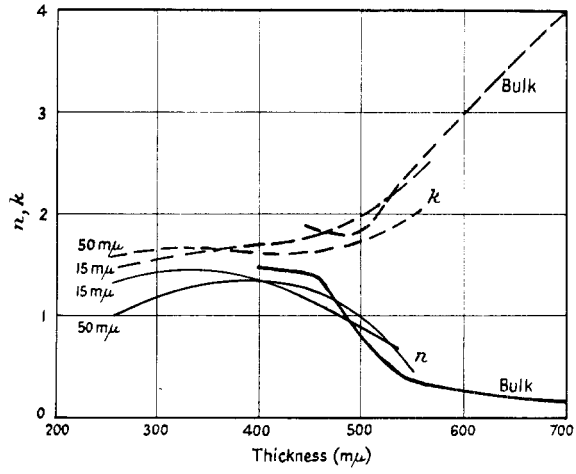

Figure 17. Dependence of optical constants on wavelength.

distribution of metal. The properties of a distribution of metal spheres embedded in a dielectric have been calculated by Maxwell Garnett (1904, 1906). The effective optical constants $\mathbf{n}_e = n_e - ik_e$ may be calculated from the constants of the constituent metal spheres. If the spheres are large enough to contain many atoms but are small in diameter compared with the thickness of the film, then $\mathbf{n}_e$ is related to the index $\mathbf{n}$ of the metal by the relation

$$\frac{\mathbf{n}_e^2 - 1}{\mathbf{n}_e^2 + 2} = q\frac{\mathbf{n}^2 - 1}{\mathbf{n}^2 + 2} \qquad \ldots\ldots(63)$$

where q is the volume fraction occupied by the spheres and the dielectric is assumed to be air. Although the calculated wavelength dependence of n_e, k_e for plausible values of q is found to show trends similar to those of the experimental results, quantitative agreement is lacking. The model is unsatisfactory for the following reasons: (i) the electron micrographs show that the metallic aggregates are not generally spherical and that their dimension normal to the film is not small compared with the average film thickness; (ii) the optical constants of such small particles will not be expected to be the same as those of the bulk since the conductivity will be considerably lowered by surface scattering. Schopper (1951), following early work by David (1939), assumes a two-dimensional distribution of spheroidal particles lying with their unique axes normal to the plane of the film. In order to obtain a fit with the experimental results it is necessary to assume that

the axial ratios of the spheroidal particles are distributed statistically about a mean value. It is convenient to work with a function f of the axial ratio b/a, calculated by David and plotted in figure 18. The axial ratios are assumed to be distributed

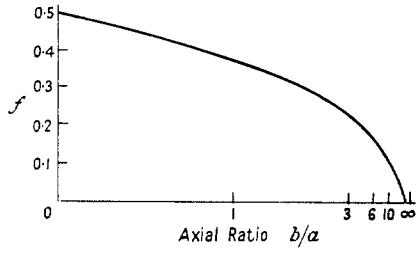

Figure 18. David's function f of axial ratio b/a.

so that the distribution function for f is given by

$$g(f) \propto f \exp(-f/\bar{f})^2. \qquad \ldots\ldots(64)$$

If d is the average film thickness and d_w the thickness deduced from the mass per unit area, then

$$\frac{d}{d_w}(n_e^2 - k_e^2 - 1) - i\frac{d}{d_w} 2n_e k_e = \bar{C} \qquad \ldots\ldots(65)$$

where

$$\bar{C} = \int \frac{[(n-ik)^2-1]\, g(f)\, df}{[(n-ik)^2-1]\, f+1} \Big/ \int g(f)\, df. \qquad \ldots\ldots(66)$$

Values of n_e, k_e are thus calculated in terms of the single parameter $\bar{f}$. The agreement between the results calculated on this model and experimental values is demonstrated in figure 19.

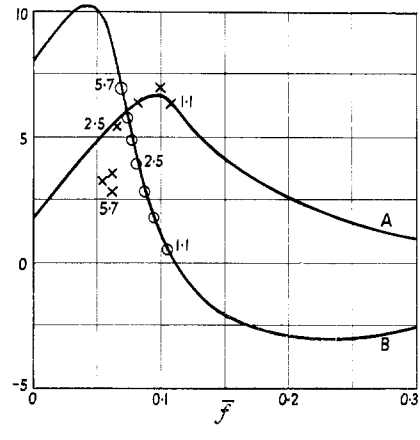

Fig. 19. Calculated and experimental results for n_e, k_e for gold films :
Curve A, $(d/d_w)\, n_e k_e$, crosses, experimental points ; curve B, $(d/d_w)(k_e^2 - n_e^2 + 1)$, circles, experimental points. Thicknesses shown in millimicrons.

Optical constants of gold in the infra-red. In investigations to determine the range of wavelengths over which the Drude free electron theory is valid, measurements have been made at wavelengths out to 15 μ (Försterling and Fréedericksz 1913, Weiss 1948, Hodgson 1955, Schulz 1957). The thicknesses of films used are generally not specified but they are opaque, or nearly so, to visible light. Their thickness is thus of the order 100 mμ or more. By the time this thickness is reached the initial convulsions of the n, k–thickness curves are complete and the limiting values reached. The aggregated structure of the films may be expected to have a smaller influence on the optical behaviour for radiation of long wavelengths than for the visible. The results are collected in figure 20. The full lines are calculated from free electron theory as modified by Reuter and Sondheimer (1948) and Dingle (1953) to allow for the anomalous skin effect.

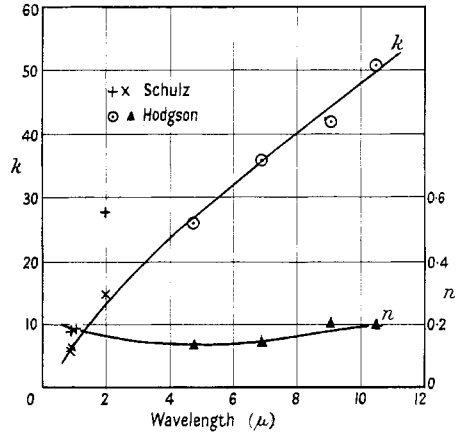

Figure 20. Optical constants of gold in the infra-red.

Homogeneity of evaporated gold films. The assumption underlying the treatments discussed above is that the properties of the film are constant throughout its thickness. Since the substrate will exercise an influence on the film structure which will diminish as the thickness increases, some gradient in properties may be expected. There is a simple relation between the absorption $\mathbf{A} = 1 - \mathbf{R} - \mathbf{T}$ for light traversing the film from the air side and $\mathbf{A}'$ for light travelling in the reverse direction. If n_s is the substrate index then for a homogeneous film $n_s \mathbf{A} = \mathbf{A}'$ (Wolter 1937). The extent to which this relation is found to hold varies considerably among different published results, indicating varying degrees of homogeneity. The departures shown by Krautkrämer's results are considerable. Fair agreement is obtained in the results of Rouard, Malé and Trompette (1953) for thicknesses up to about 15 mμ beyond which the departures become large. This test of homogeneity cannot be applied to Schulz's results since the films used for the measurement of n are opaque. The criterion applied by Schulz, that the ratio R_s^2/R_p be unity, may be less sensitive as a detector of a gradient in properties normal to the surface since both measurements are made on the same side of the film. On the other hand, for thick films such as were used by Schulz, the effects of the substrate may be felt in only a small fraction of the film thickness.

The optical behaviour of gold films deposited at oblique incidence has been studied by Reimer (1957): such films show a marked dependence of transmission on the direction of polarization relative to the evaporation direction for the film. This behaviour is associated with a structure asymmetry, clearly shown in electron micrographs of the films. Similar properties are exhibited by films of Ag, Cu and Mn.

The properties of gold films sputtered on to bismuth oxide. The differences in behaviour between films of gold produced by evaporation and that calculated for a plane, parallel-sided layer with optical constants appropriate to bulk gold are reasonably well explained in terms of the granular structure of such films. The work of Gillham, Preston and Williams (1955) on sputtered gold films deposited on sputtered bismuth oxide shows that it is possible to produce films of thickness tens of millimicrons with properties closely similar to those of bulk gold. It appears that the adhesive forces between gold and bismuth oxide are sufficiently large to overcome the tendency, produced by surface tension forces, for the film to aggregate. After suitable annealing treatment the films are found to possess electrical conductivities within about 30% of that of the bulk metal, in contrast to the behaviour shown by evaporated films. The optical constants of the films sputtered on bismuth oxide are found to be much more nearly like those of the bulk than are those of evaporated films. Electron micrographs of the sputtered films reveal continuous sheets of monocrystalline lamellae, each of lateral dimensions some ten times the mean film thickness.

6.1.2. *Silver films.*

Dependence of optical constants on thickness. There is considerably greater variation between different observers' results than in the case of gold films, probably arising from the greater reactivity of the metal, with the greater chance of contamination. There is some doubt about the figures quoted by Krautkrämer (1938), obtained by the procedure given by Murmann (1933, 1936) since this method does not give unique values of n and k. The wrong values may have been chosen.

Extensive measurements by Philip and Trompette (1957) on films up to 70 mμ in thickness and for wavelengths ranging from 302 mμ to 578 mμ show a behaviour generally similar to that shown by gold. High values of n and low values of k at small thicknesses (figure 21) tend gradually with increase of thickness to values in the neighbourhood of those recorded for the bulk metal. Analysis of the results using the Maxwell Garnett theory shows that the general features of the film behaviour are accounted for by its granular structure although, since the model is somewhat crude, the agreement is not close. Figure 21 also records the results obtained by Clegg (1952) for silver films on which the measurements were made in vacuum. The large difference between the two sets of results quoted suggests that a detailed analysis of results of this kind is better postponed until more effective control of conditions obtains.

Dependence of optical constants on wavelength. Measurements on thick silver films, annealed until the $R_s^2 = R_p$ criterion shows them to be homogeneous, were made by Schulz (1954 a) and Schulz and Tangherlini (1954) using the methods described in § 5. Whilst agreement with earlier (bulk) values of k was obtained, significantly lower values of n emerged. The measurements were made at the

glass–silver interface and were therefore less subject to uncertainties from contamination than those made on films exposed to air. For wavelengths from 1 to 3 microns the values of k are as expected from the Drude free electron theory, when the anomalous skin effect is allowed for. Departures observed in the earlier

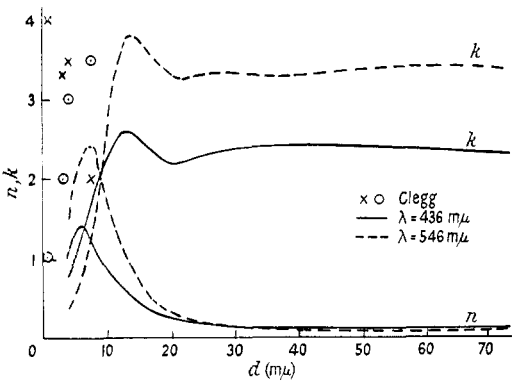

Figure 21. Optical constants of silver films.

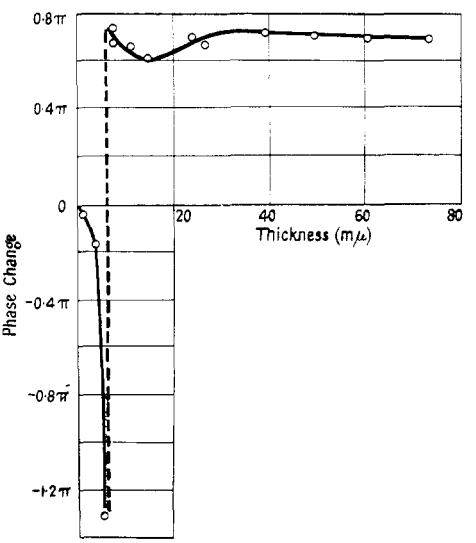

Figure 22. Phase changes on reflection at silver films.

results of Försterling and Fréedericksz (1913) are ascribed to contamination since these measurements were made on air-exposed surfaces. Recent measurements of reflectance in the region 1–13 μ by Gates, Shaw and Beaumont (1958) suffer from the same disadvantage. Since non-normal incidence and unpolarized radiation were used, the results cannot be readily interpreted. Some scatter is shown in the results for the region 1–10 μ by Beattie and Conn and Hodgson (see Schulz 1957), reflecting the difficulties attendant in this spectral region, but the values of k are substantially as expected on the Drude theory.

Homogeneity of evaporated silver films. Extensive measurements on the phase changes on reflection at films of silver (Avery 1950, Faust 1950, Clegg 1952, Philip 1956, Dumontet, Perrot and Tortosa 1957, Lisitsa and Tsvelykh 1957) reveal a highly complex variation of this quantity with film thickness and with wavelength. For some wavelengths a phase jump of 2π (figure 22) is observed for a thickness generally below 10 mμ. At other wavelengths no such jump is found. This behaviour cannot be interpreted in terms of a single homogeneous film and measurements by Dumontet *et al.* suggest that a transition layer at the surface could be the cause of the anomalies. The results of phase change measurements made on silver surfaces exposed to air are of considerable importance to interferometry : it is unlikely that a detailed study of the adventitious contamination which gives rise to these anomalies is worth while.

A summary of results of optical constant measurements on thick silver films at various wavelengths is given in Appendix II.

6.1.3. *Other metals.*

Alkali metals. Measurements of the optical constants of (unspecified) thick films of potassium, sodium, rubidium and caesium have been made by Ives and Briggs (1936, 1937 a, b) for wavelengths from 200 mμ to 650 mμ. The films were condensed on quartz and sealed against atmospheric contamination by

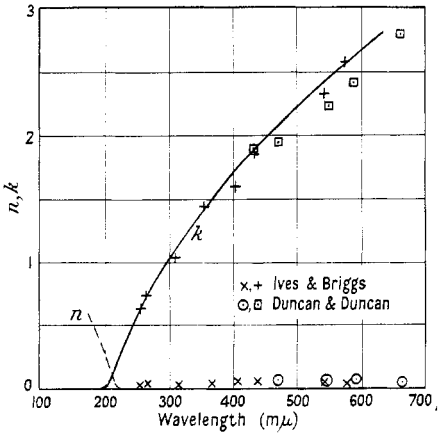

Figure 23. Optical constants of sodium. Curves calculated from Kronig theory.

paraffin wax, measurements being made at the quartz–metal surface. The results are found to agree reasonably well with those calculated on the basis of Bloch's theory of metallic conduction, with the assumption that collisions between electrons and the atoms of the lattice may be neglected (Kronig 1931). Dispersion curves for sodium are shown in figure 23 together with early measurements of Duncan and Duncan (1913). Collected values of n and k for the alkali metals are given in Appendix II.

Aluminium. In the far ultra-violet region of the spectrum the reflectance of aluminium is among the highest known. On account of their importance in spectroscopic work, the properties of Al films have been carefully studied in this

region (Hass, Hunter and Tousey 1956, 1957, Gerharz 1958). The speed of evaporation has a pronounced effect on the reflectance, particularly in the region $\lambda = 160$ mμ to 180 mμ, the highest reflectance being obtained for rates of deposition in excess of 30 mμ sec^{-1}. No marked dependence on pressure in the neighbourhood 10^{-5} to 10^{-4} mm Hg is observed. The dependence of reflectance on film thickness for various wavelengths is shown in figure 24. A fall in reflectance is observed on ageing and is shown to be a consequence of the formation of aluminium

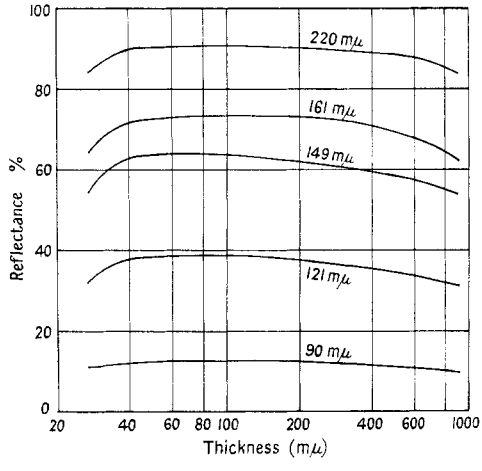

Figure 24. Dependence on thickness of ultra-violet reflectance of aluminium films. Wavelengths marked on curves.

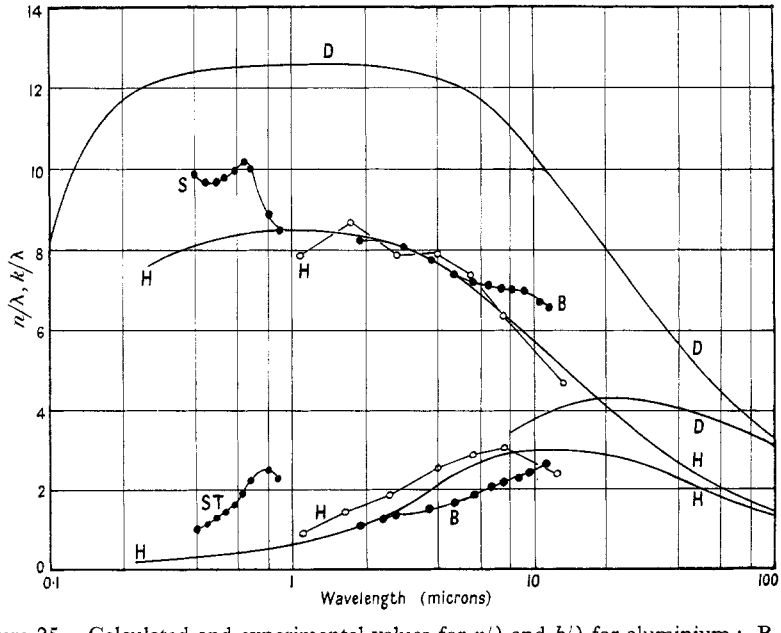

Figure 25. Calculated and experimental values for n/λ and k/λ for aluminium : B, Beattie 1955 ; H, Hodgson 1955 ; ST, Schulz and Tangherlini 1954 ; S, Schulz 1954 a ; D, Drude theory.

oxide on the surface. The optical constants of aluminium and aluminium oxide in this region, determined by reflection measurements, are given in table 1.

Table 1. Optical Constants of Al and Al_2O_3 in the Ultra-violet

Wavelength (mμ)		90	122	220
Aluminium	n	0·55	0·37	0·14
	k	0·60	0·94	2·35
Aluminium oxide	n	1·30	1·75	1·85
	k	0·87	0·72	0·00

In the visible region, early results of O'Bryan (1936) are substantially confirmed by Schulz and Tangherlini (1954) and Schulz (1954 a). Measurements in the near infra-red by Hodgson (1955) and Beattie (1955) show that, although the results agree with predictions of the Drude theory on the basis of approximately 1·3 electrons per atom (figure 25), this assumption leads to incorrect behaviour at very long (100 μ) wavelengths, at which the classical skin effect would be expected to apply.

Copper. The variation with film thickness of the optical constants of copper films (figure 26) is similar to that shown by silver and gold. The limiting values

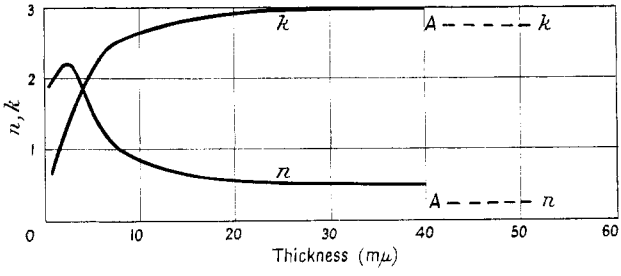

Figure 26. Optical constants of copper for $\lambda = 586$ mμ. A, Avery's results on thick films.

to which n and k tend for sputtered films differ appreciably from those obtained for thick (40–50 mμ) evaporated films (Avery 1950). Results of measurements by Schulz (1954 b) on thick films show that a fit may be obtained at long wavelengths with the Drude theory provided that the ratio of effective to normal electron mass is taken as 1·45. This value agrees with that obtained from electronic specific heat determinations. Values of m^*/m deduced from the measurements of Beattie and Conn (1955) in the near infra-red yield a considerably higher value, suggesting that bound electrons may be playing a part in the absorption. There is some considerable difference between Beattie and Conn's results and those of Hodgson (1955), presumably due to some difference in experimental conditions.

Platinum and palladium. Early measurements on sputtered films of these metals show the usual trends of n and k with film thickness. More recent work of Malé and Trompette (1957) on Pd films formed by thermal evaporation (pressure 10^{-5} mm Hg, rate of deposition 10 mμ min^{-1}) are interpreted in terms of film granularity. From the mass thickness d_m and the figure deduced optically d_o, the *coefficient de remplissage* $q = d_m/d_o$ is determined. Values of q obtained for

several different wavelengths (302 to 546 mμ) are found to agree, thus validating the procedure adopted for this metal. The optical constants are found to increase monotonically with thickness for all wavelengths. The dependence of q on the thickness d_0 is shown in figure 27 and reveals a very large extent of voids in the thinner films. In analysing the above results in terms of dispersion theory Grard (1957 a) concludes that there are no resonant frequencies over the wavelength range examined, in contrast to those observed for gold and silver (Grard 1957 b, c).

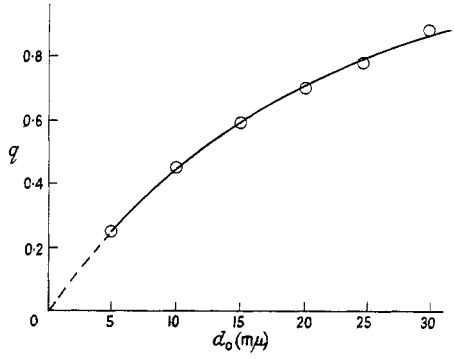

Figure 27. Dependence of q on thickness for Pd films.

This conclusion may be valid although no account is taken of the variation of optical constants arising from the granular structure of the films. In the thickness range covered (5 to 30 mμ) a marked dependence of n and k from this cause is observed.

Tin. Measurements of n and k for 2·5 mμ tin films have been compared with those calculated on the basis of the Maxwell Garnett theory. Reasonable agreement is obtained: the q-value is not stated.

Table 2. Optical Constants of Tin Films. Thickness 2·5 mμ

Wavelength	356 mμ		546 mμ	
	n	k	n	k
Experimental	2·3	1·0	3·0	0·5
Calculated	2·2	1·5	2·8	0·3
Bulk metal	—	—	1·0	4·2

Measurements by Hodgson (1955) on thick tin films in the infra-red show departures from the free electron behaviour at wavelengths below about 5 μ. No account is taken of the highly granular structure which is observed even in very thick films and this might well account for the departures from theory which treat the film as a continuum.

Lead. Measurements of the optical constants of lead films *in vacuo* and in air (Trompette 1959) show the usual trends suggestive of a granular structure, the values of q ranging from 0·49 to 0·82 for films of thickness up to 35 mμ. Whilst the optical behaviour of these films for visible wavelengths changes but little on exposure to air, the ultra-violet absorption rises considerably. This is rather strange in view of the fact that the conductivity of the films decreases for

thicknesses below 65 mμ. The reason for this is not clear. The effect of oxidation on the optical properties is found to occur practically instantaneously suggesting that a completely protective oxide film forms.

Tantalum, tungsten, zirconium and silicon. These metals prove of particular interest in the far ultra-violet where their reflecting properties approach that of aluminium. Measurements by Fabre and Romand (1956) on films formed by evaporation (15 minutes' evaporation for a film transmitting approximately 1% of visible light) are shown in figure 28. The curve for tungsten refers to a freshly

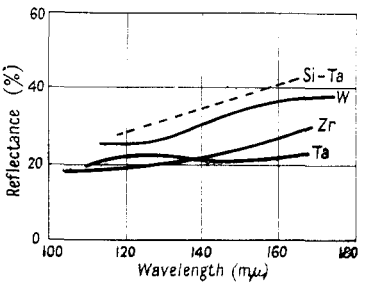

Figure 28.

Reflectance of films of Ta, W and Zr. Broken line: Si film contaminated with tantalum.

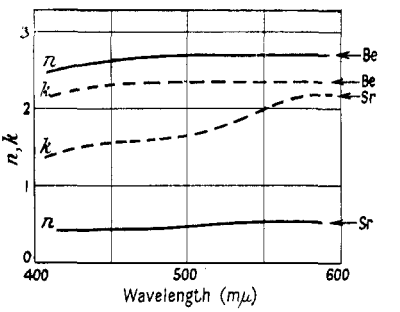

Figure 29.

Optical constants of Be and Sr.

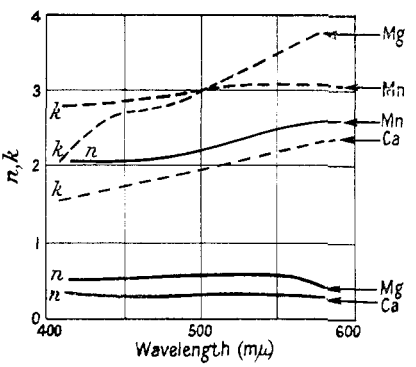

Figure 30.

Optical constants of Ca, Mn and Mg.

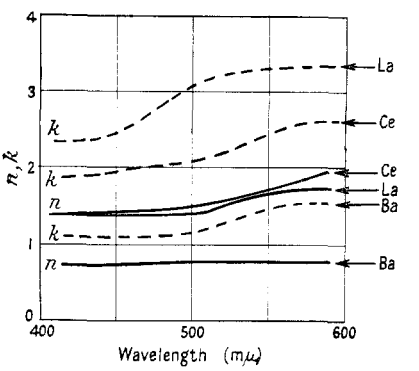

Figure 31.

Optical constants of Ba, Ce and La.

deposited film: on exposure to air a considerable fall in reflectance results. Although the reflectance of Si films in this region is about 10%, that of films formed by high-temperature evaporation from a Ta boat is very high (figure 28) (Kandare and Fabre 1956).

Mg, Be, Ca, Ba, Sr, La, Mn and Ce. O'Bryan (1936) has measured the optical constants of these metals for the principal lines of the mercury spectrum in the visible: the results are collected in figures 29–31. The films were all produced by thermal evaporation.

6.2. *Dielectric Films*

The optical behaviour of dielectric films is in some ways simpler than that of metal films. Whereas metal films show near-dielectric properties in very small

thicknesses, on account of the effects of granularity, in a dielectric film this feature simply results in a decreased refractive index. The effects of granularity in structure and of inhomogeneity are however detectable, as illustrated by the results obtained for cryolite and calcium fluoride discussed below. Films produced by thermal evaporation will be discussed first followed by those produced chemically or electrolytically.

6.2.1. *Films formed by thermal evaporation.*

Calcium fluoride. A detailed study by Bousquet (1956) of the reflectance and transmittance of CaF_2 films, deposited by thermal evaporation (10^{-5} mm Hg) on glass and quartz, reveals that such films are anisotropic and exhibit a *couche de passage* at the film–air surface. For a uniform film whose index is lower than

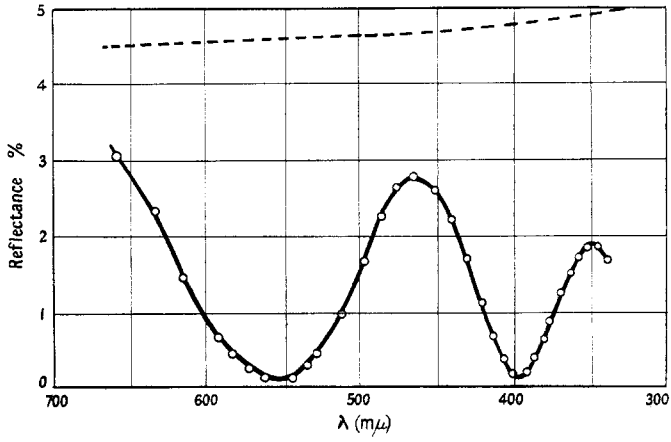

Figure 32. Reflectance–wavelength curve for evaporated CaF_2 films. Broken curve: reflectance of bare substrate.

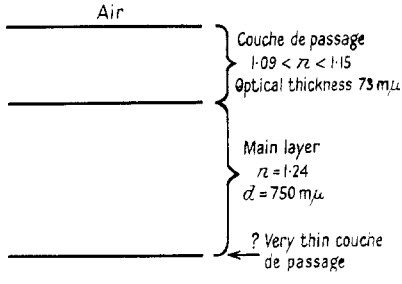

Figure 33.

that of the substrate and of optical thickness $k\lambda/2$ the reflectance should exhibit maxima equal to the reflectance of the bare substrate. The spectrophotometric curve for a film of optical thickness 690 mμ on glass is shown in figure 32. The maxima lie well below the values for the bare substrate. The transmittance curve is found to be complementary, within the accuracy of the measurements (to $\pm 0{\cdot}3\%$), showing that the departure from the behaviour expected of a uniform film cannot be ascribed to absorption. Figure 33 shows the form of layer which would yield

the reflectance curve of figure 32. When monochromatic light is totally reflected at a glass–CaF_2 interface, fringes are observed in the neighbourhood of the critical angle, consistent with the diffusion of light by the film at angles other than the apparent angle. A study of the contrast observed in the fringe system suggests that these films are anisotropic, a conclusion amply confirmed by phase change measurements at angles near the Brewster angle (Bousquet and Delcourt 1957). The magnitude of the birefringence is found to depend on the angle of arrival of the condensing atoms (Sinelnikov, Shkliarevsky and Vlasenko 1957) the maximum birefringence observed being about 0·03. Films of fluorite deposited at oblique incidence on a rotating surface are found to show marked optical activity (Young and Kowal 1959), the rotation for films 18 μ thick ranging up to the order 2°. Films deposited obliquely on to a fixed substrate show birefringence with an optic axis inclined to the film normal. On a film formed on a rotating surface a helical anisotropy results.

Cryolite (Na_3AlF_6). Similar behaviour is observed to that for CaF_2 except that the reflectances at maxima are higher than those of the bare substrate. The

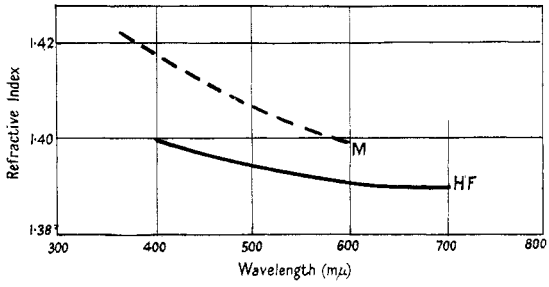

Figure 34. Dispersion of MgF_2 films. HF, Hall and Ferguson 1955 a ; M, Morita 1956.

march of the reflectance–wavelength curves measured at various angles of incidence around the Brewster angle is markedly different from that calculated for a uniform film and is suggestive of a *couche de passage* at the film–air interface. The mean value of the refractive index of the whole film (λ = 486 mμ) is 1·375.

Magnesium fluoride. Since this material is widely used as an anti-reflecting coating on glass, its properties have been extensively studied (Bannon 1946, Rood 1949, Abelès 1950, Schulz and Scheibner 1950, Heavens and Smith 1957, Sanford 1958). Reflectance measurements by Bousquet (1956) indicate that, unlike CaF_2 and cryolite, the departures from homogeneous behaviour are relatively small. Since the values obtained for the refractive index lie close to (in fact, *above*) those quoted for the mineral sellaite, the films probably contain few voids.

Refractive index measurements by Hall and Ferguson (1955 a) and by Morita (1956) are shown in figure 34 for films of 200 to 800 mμ thickness. Electron micrographs of MgF_2 films show them to be exceedingly fine-grained (Morita 1957). Loss by scattering in films formed on glass is found to be less than 1% : on heated quartz, a loss of several per cent is observed, arising from the formation of cracks in the film. MgF_2 films are found to be in a state of high tensile stress which increases with thickness and may cause disruption of the film at thicknesses beyond 2 μ. In the ultra-violet region of the spectrum, the refractive index is

found to depend more markedly than in the visible on the film thickness and rate of deposition. Marked inhomogeneity is detected (Hall 1957), especially in rapidly deposited layers of thickness a few tens of millimicrons. Absorption in the films—negligible in the visible—rises steeply for wavelengths below 230 mμ ($k \sim 0{\cdot}005$ at $\lambda = 210$ mμ).

Lithium fluoride. In studies of thick (2–18 μ) films of LiF Schulz (1949) finds that the proportion of solid LiF in the films rises from 70 to 82%. The voids are mainly accessible to a filling liquid although as the thickness increases over the above range the proportion of inaccessible voids rises to about 3%.

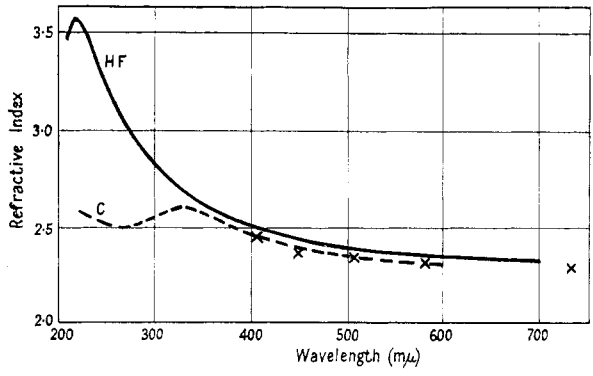

Figure 35. Refractive index of ZnS films. HF, Hall and Ferguson 1955 a ; C, Coogan 1957 ; crosses, Kuwabara and Isiguro 1952.

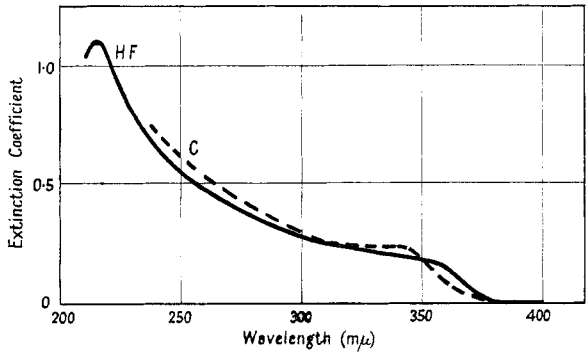

Figure 36. Extinction coefficient of ZnS films. HF, Hall and Ferguson 1955 a ; C, Coogan 1957.

Zinc sulphide. The popularity of this material as a high-index component in multilayers, before being largely ousted by cerium dioxide, has resulted in many studies of its properties (Hammer 1943, Shalimova 1951, Hall and Ferguson 1955 a, b, Hall 1956, Coogan 1957). Over the region 400 mμ to 700 mμ there is reasonable agreement between different results, showing a decrease in index from 2·5 at 400 mμ to 2·3 at 700 mμ. Most of the values obtained for films are slightly below ($\sim 0{\cdot}1$) those for the bulk crystal. Below 400 mμ there are large differences, both between different observers' film results and between film and bulk values

(figure 35). Hall records a steady increase in n as λ falls to 225 mμ, at which wavelength $n = 3{\cdot}6$. Coogan's results show a maximum (2·6) at 350 mμ and a minimum (2·5) at 290 mμ. Fair agreement is shown in the results for the extinction coefficient (figure 36). It is suggested that the enhanced absorption in the neighbourhood of 330 mμ may indicate an exciton band. From 2 μ to 14 μ the refractive index of ZnS films falls steadily from 2·25 to 2·15 : the extinction coefficient is less than approximately 0·001 in this region.

Huldt and Staflin (1959) obtain a significantly higher index ($\sim 2{\cdot}37$ at $\lambda = 1{\cdot}5$ μ) for films prepared with residual air in the evaporation chamber than for those produced with residual nitrogen ($n \sim 2{\cdot}28$). Similar behaviour is shown by germanium films.

X-ray studies indicate that ZnS films deposited on glass substrates at room temperature are mainly amorphous.

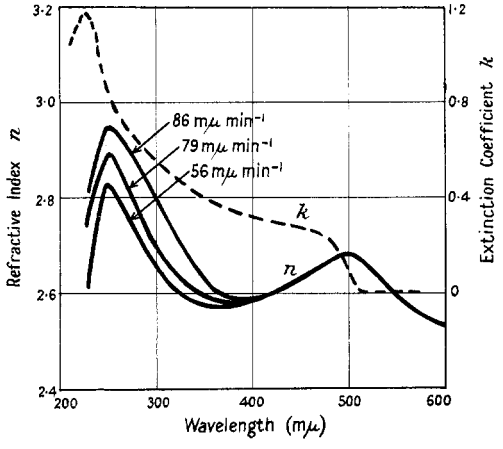

Figure 37. Dependence of refractive index of CdS films on rate of deposition. Full lines, refractive index ; broken line, extinction coefficient.

Cadmium sulphide. The optical behaviour of CdS films is found to depend on the rate of deposition, low rates favouring low optical absorption and low refractive index (figure 37). Considerable care is needed if spurious high absorption, due to dissociation, is to be avoided. Hall and Ferguson evaporate the material from a filament in contact with the charge. The filament temperature must not exceed 1025° C. In the region 1–4 μ, the extinction coefficient is a minimum, ranging from approximately 0·01 for a deposition rate of 40 mμ min^{-1} to approximately 0·05 at 200 mμ min^{-1}. (It seems likely that this variation will be due to dissociation.) From 2 μ to 14 μ, the refractive index falls slightly from 2·30 to 2·25. Beyond 7 μ, k is no longer influenced by the rate of deposition. The films show the cubic structure of CdS.

Cerium dioxide. The high refractive index and robust mechanical properties of CeO_2 films make them very suitable for high-reflecting multilayers (§ 8.2) in place of ZnS. The conditions necessary for obtaining reproducible, stable properties have been investigated by Hass, Ramsey and Thun (1958). The crystallite size (figure 38) and refractive index (figure 39) depend markedly on the

substrate temperature. Before evaporation, CeO_2 powder is baked and sintered in air at 1100° c : furthermore the evaporation charge must be pre-heated to the evaporation temperature before deposition is allowed to begin. CeO_2 films show considerable absorption ($R = 0{\cdot}41$, $T = 0{\cdot}24$, $A = 0{\cdot}35$) at $\lambda = 320\,\mathrm{m}\mu$. At 500 m$\mu$ and above the absorption is negligibly small ($< 0{\cdot}1\%$ in $\lambda/4$ layers).

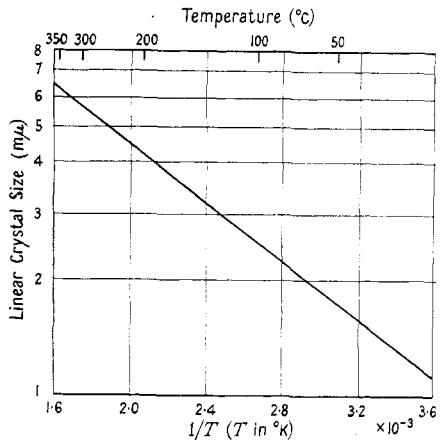

Figure 38. Crystallite size of CeO_2 films as function of substrate temperature during deposition.

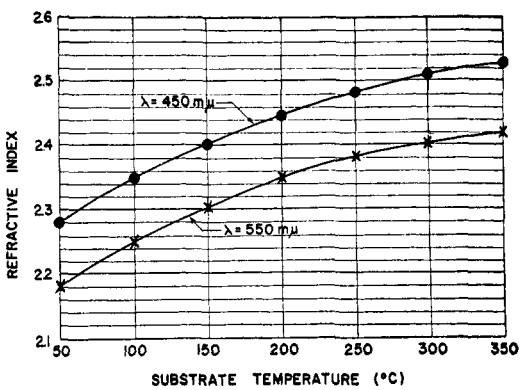

Figure 39. Dependence of refractive index of CeO_2 films on substrate temperature.

Antimony sulphide. The few results obtained for this material show such wide differences that only brief mention is made here. Schopper (1952 b) obtains $n = 2{\cdot}5$, $k = 0{\cdot}01$ for $\lambda = 640$ mμ and $n = 2{\cdot}6$, $k = 0{\cdot}29$ for $\lambda = 436$ mμ. These are significantly lower than values reported by Kunze (1958) who finds a maximum (3·4) at 680 mμ falling to 2·7 at 500 mμ and 1·5 μ. These are in turn lower than the results of Billings and Hyman (1947) : $n = 3{\cdot}0$ at $\lambda = 589$ mμ. There seems some doubt over the optical constants of the mineral stibnite although the values quoted are very much higher than those obtained on films (Hutchinson 1907, Bailly 1938).

Silicon monoxide (Hass and Salzburg 1954). In order to form films of SiO by evaporation, a high rate of deposition (> 1 mμ sec^{-1}) is needed at a pressure less than

10^{-5} mm Hg ; the source temperature should be approximately 1200° c. Unless these conditions are met there is a tendency for the higher oxide to form. (Since the absorption of SiO_2 in the ultra-violet is lower than that of SiO, the oxidized film is more suitable as a protective film in this region.) The optical constants of (true) SiO films of thickness 30–2000 mμ are shown in figure 40. The absorption peak at 10 μ results in a decrease in reflectance of an aluminium film with protective SiO coating if too large a thickness of SiO is used. For a protective film 125 mμ thick the decrease amounts to only 1–2% (the transmission of a rocksalt plate is, however, reduced by about 20%).

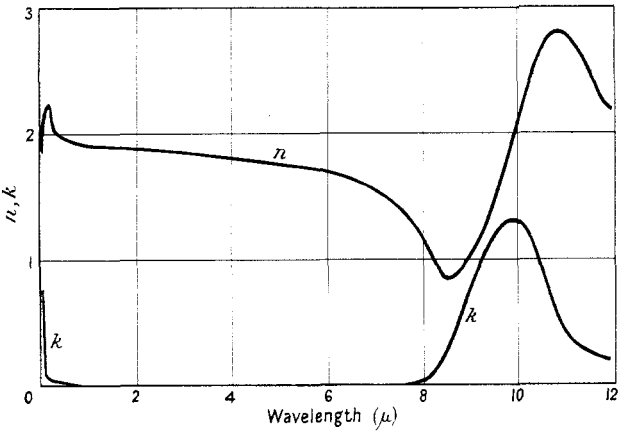

Figure 40. Optical constants of SiO films.

An interesting property of films formed by evaporating SiO is the wide range of refractive indices which can be obtained by varying the evaporation conditions. In the wavelength range 500 to 700 mμ indices from 1·55 to 2·00 may be obtained. The mechanical properties of the films are satisfactory.

6.2.2. *Chemically and electrolytically deposited films.*

Titanium dioxide. Films formed by the direct evaporation of TiO_2 are found to be heavily absorbing, indicating that some decomposition takes place. Transparent films may be produced either by allowing fuming $TiCl_4$ to decompose on heated glass (Banning 1947) or by thermal oxidation of titanium films formed by evaporation (Hass 1952). Films formed by oxidizing Ti at 400° c for several hours are found to consist of the rutile form of TiO_2. The measured dispersion of the films follows closely that of bulk rutile, the film values being consistently about 0·05 below the bulk figures. Over the wavelength range 400 to 2000 mμ the absorption of $\lambda/4$ films is less than 0·5%. The refractive index falls steadily from 3·00 at 400 mμ to 2·50 at 2000 mμ. Films formed by the decomposition of $TiCl_4$ vapour on glass at temperatures below 280° c are found to be amorphous : at higher substrate temperatures the anatase form of TiO_2 is produced. The refractive index of these films ranges from 2·4 (450 mμ) to 2·25 (700 mμ). They are rougher and mechanically less durable than those made by oxidizing metallic Ti films.

Aluminium oxide. Transparent, non-porous films of aluminium oxide can be prepared (Hass 1949) by anodizing in a solution of ammonium tartrate. The films grow to a limiting thickness determined by the applied voltage. This thickness is approximately 1·3 mμ volt^{-1}, depending to some extent on the state of the aluminium surface before anodizing (van Geel and Schelen 1957). The exact nature of the films is uncertain : since they are amorphous, identification by x-ray means is not possible. The observed refractive index ($\sim$1·6 for λ = 589 mμ) lies well below that of bulk Al_2O_3 (1·76) ; also the density is found to be 3·1 g cm^{-3} whereas that of the bulk is 3·42 g cm^{-3}. Refractive index measurements by Weisskirchner (1951) reveal an increase with anodizing voltage for measurements at 589 mμ. Harris (1955) observes the reverse tendency in measurements made out to 15 μ (figure 41). The extinction coefficient shows an absorption band near

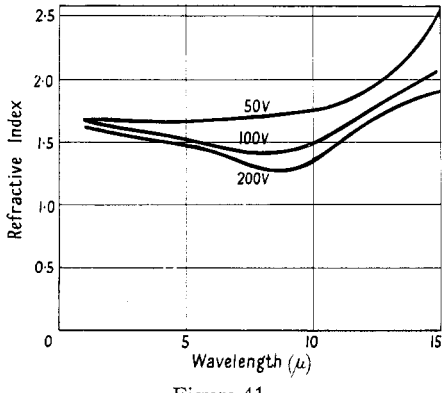

Figure 41.

Dispersion of anodic aluminium oxide films. Anodizing voltage shown on curves.

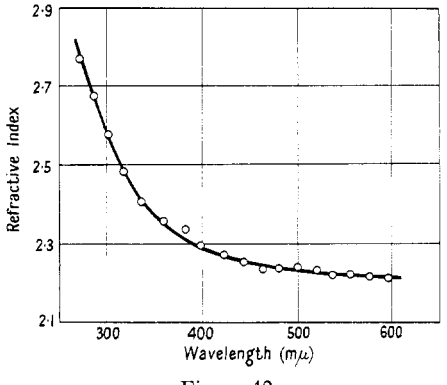

Figure 42.

Dispersion of anodic Ta_2O_5 films.

15 μ ; values of k are scarcely affected by the anodizing voltage. The refractive index results suggest that there may be a dependence of film composition or structure on thickness. That there is some uncertainty over the structure is shown by measurements by Kelly (1958 b) of the volume ratio of the oxide : this is found to depend on the age of the electrolysing solution.

Tantalum oxide. The most recent results on the refractive index of anodic tantalum oxide (Young 1958) are shown in figure 42. The index at 590 mμ was determined by immersion: the indices relative to this value were found from spectrophotometric curves. In so far as the correct procedure is adopted in allowing for phase changes on reflection at the interfaces, these results are correct for the average index of the films. There is some evidence (Heavens and Kelly 1958) that these films show a gradient of index throughout their thickness.

Reactively sputtered oxides. Films of certain metal oxides may be produced by sputtering the metal in a cathodic discharge in the presence of oxygen—a process known as reactive sputtering. Such films are generally semiconducting with a reasonably high (from $\sim$100 ohms per square) conductivity : many are non-absorbing in some parts of the visible spectrum. Details of the methods of preparation and of the optical and electrical properties of iron oxide, indium oxide, tin oxide and cadmium oxide are given by Holland and Siddall (1953).

§ 7. Methods of Controlling Film Thickness

In many of the applications of thin films to optical systems discussed below it is necessary to deposit films of accurately determined thickness. Several methods for achieving this are available. The nature of the problem is such as to require methods which can be employed during the deposition of the film : both polarimetric and spectrophotometric methods can be used.

7.1 *Semi-reflecting Metal Films*

In certain types of filter, partly reflecting metal films are used although in many instances these would now be replaced by multiple dielectric layers. The thickness of the metal layers is generally not highly critical and it suffices to monitor their thickness by measurement of the transmitted light intensity. For opaque films, resistance measurements may be used. An accuracy to 3–4% is easily attained and is generally sufficient.

7.2 *Dielectric Layers*

Visual observation of the colour changes in light reflected from a dielectric layer during deposition enables multiple quarter-wave layers to be deposited with an accuracy to perhaps 10% : for some purposes, e.g. single anti-reflecting coatings, this is sufficient. If a monochromatic source and photocell are used, preferably with a recording meter, then the positions of maxima and minima in the reflectance curve can be located to within $\pm 2\%$ (Jarrett 1952, Heavens 1955). This accuracy is adequate for the preparation of high-reflecting multilayer stacks. For the production of interference filters, in which the position of the passband depends critically on the layer thickness, a higher accuracy is needed. The method introduced by Giacomo and Jacquinot (1952) entails illuminating the system with a beam whose wavelength scans over a small range with frequency f. If the light passes through a film of thickness $m\lambda/4$, where λ is the mean of the scanning wavelength range, then the photocell output will contain no signal of frequency f. If λ corresponds to a point of inflection on the transmission curve of the film a zero at frequency $2f$ is obtained. This method has been further developed by Lissberger and Ring (1955) and yields an accuracy to ± 1 mμ in the position of the passband of a second-order interference filter (§ 8.3) and to $\pm 1{\cdot}5$ mμ in that of a first-order filter. A simple experimental arrangement using colour filters is described by Traub (1956) in which duplication of a given film of the correct thickness is achieved to within a small fraction of one per cent.

Polarimetric methods have been employed by Hermansen (1955) and by van Heel and Walther (1958). Hermansen reflects plane polarized light at an angle of 75° and measures the differential phase change $\Delta = \delta_p - \delta_s$. For suitably chosen wavelengths an accuracy to ± 1 mμ is obtained. The normal incidence method of van Heel and Walther (§ 5.2) using a Savart plate is experimentally somewhat more convenient : the accuracy attainable is to ± 2 mμ.

7.3 *Piezoelectric Crystal Method*

In a recent and novel method by Lostis (1959) the change in frequency of an oscillating quartz crystal is measured when a film is deposited on its surface. The frequency difference between that of the test crystal and of a standard is measured

using an ordinary counter-type frequency meter. For a resonant frequency of 5 Mc/s the frequency change can be easily measured to within ± 1 c/s. For a crystal of mass M_0 of resonant frequency f_0 the frequency change Δf for a film of thickness Δe and density ρ is given by

$$\frac{\Delta f}{f_0} = \rho \frac{\Delta e}{M_0}. \qquad \ldots\ldots(67)$$

For an aluminium film for example a thickness of 1 mμ produces a change of 3 c/s indicating that the method is capable of an accuracy to about $\pm 0{\cdot}3$ mμ.

§ 8. Some Applications of Thin Films in Optics

The number and diversity of applications of thin film techniques is prodigious and is increasing rapidly. No attempt is made to be comprehensive ; details are given of results which serve to illustrate the type of system which can be achieved with existing materials and methods.

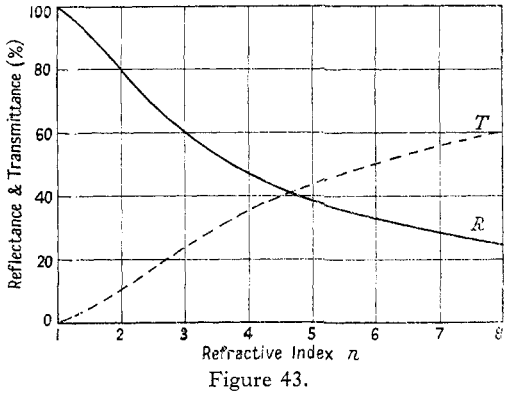

Figure 43.

Reflectance and transmittance of parallel-sided (thick) slab for different refractive indices.

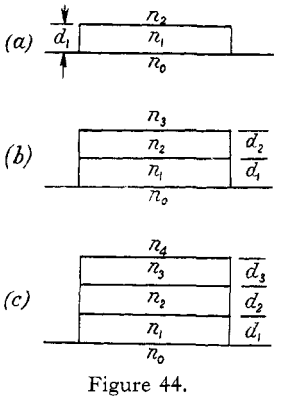

Figure 44.

Typical anti-reflection systems. $n_1 d_1 = n_2 d_2 = n_3 d_3 = \lambda/4$.

8.1 *Anti-reflecting Systems*

In some circumstances the loss of light by reflection at the surfaces of the optical elements of a system can be serious. Figure 43 shows the transmittance of a plane parallel-sided slab of non-absorbing material as a function of refractive index : indices as high as 4–5 are commonly met in optical systems in the near infra-red.

For reducing reflection in the visible spectrum magnesium fluoride offers a satisfactory compromise between anti-reflecting properties and durability. The colour effects likely to result when many elements of a system are coated with MgF_2 layers have been investigated by Murray (1956). Double and triple layer anti-reflecting systems may be designed to reduce reflectance to zero at two and three wavelengths (Lockhart and King 1947, Turner 1950). For the systems shown in figure 44 the relations to be satisfied for zero reflection are as follows :

(*a*)	$n_1^2 = n_0 n_2$		.....(68)
(*b*)	$n_2^2 n_0 = n_1^2 n_3$	(single zero)	.....(69)
(*c*)	$n_1 n_2 = n_0 n_3$	(two zeroes)	.....(70)
(*d*)	$n_2^2 = n_1 n_3 = n_0 n_4$	(three zeroes).	.....(71)

The positions of the multiple zeroes with respect to λ_0 are determined by the values of the indices chosen (equations (69)–(71) determine only the *ratios* of the indices). In particular, for the three-layer system, the outer zeroes lie symmetrically about λ_0 if $n_1^2 = n_0 n_2$ and $n_3^2 = n_2 n_4$: this system gives effective reduction of reflectance over a wavelength range three times that for a single film.

If an electronic computer is available approximate methods for obtaining a desired reflectance curve may be used similar to that described in § 8.2.3 for a broad-band reflecting system. The curves for a given set of indices and thicknesses may be computed directly from equation (38). Approximate expressions for 2-, 3- and 4-layer anti-reflecting systems have been given in closed form by Thelen (1956) and by Kard (1957 b). For systems containing no high-index layers, simple graphical methods in which multiple reflections are ignored serve to indicate the general behaviour.

Systems used in the near infra-red.

For plates required to transmit well over a fairly narrow ($\sim \lambda/3$) region, a single quarter-wave film suffices. An increase of 5–10% in the transmittance of quartz, flint glass, MgO and sapphire plates (Jeness 1956) by the use of $\lambda/4$ MgF_2 and LiF layers is reported. In figure 45 are compared the transmission of a silicon plate (1·5 mm) with and without anti-reflecting layers of SiO, evaporated to give a refractive index of 1·90 (Cox and Hass 1958). For longer wavelengths ZnS has been used. The effectiveness of a thin InSb slab as a cut-on filter is greatly improved (Smith and Moss 1958) by anti-reflecting films of $PbCl_2$ (figure 46).

For plates which are required to operate over wider ranges two- and three-layer coatings have been used. Reflection and transmission curves for glass with (*a*) a single MgF_2 layer and (*b*) a $SiO + MgF_2$ pair are shown in figure 47 (Cox, Hass and Rowntree 1954). Arsenic trisulphide glass may be effectively bloomed by $\lambda/4$ cryolite + $\lambda/4$ tungsten oxide layers resulting in an improved transmission from 1·6 to 8 μ (apart from an absorption band at 3 μ, possibly due to water in the films). Triple-layer blooming of Ge, with stibnite (2·8), tin oxide (1·9) and thorium fluoride (1·5) yields more than 90% transmission from 3·5 μ to 10 μ, in contrast to 45% for the uncoated plate (figure 48) (Hass and Turner 1957).

8.2 *High-reflecting Systems*

8.2.1. *Protected metal mirrors.*

By the use of suitable thicknesses of transparent protective films on metal mirrors the reflectance may be increased over part of the spectrum. The use of SiO as a protection for Al has been mentioned above: it should be noted that whereas the absorption of a 125 mμ SiO film on a transparent window (e.g. NaCl) is considerable at some wavelengths, the effect on reflection from a metal mirror is negligible. This follows from the fact that a node forms at the metal surface: for wavelengths much greater than the optical film thickness the energy absorbed under this condition is very small. Protection and enhancement of reflection can be effected by quarter-wave pairs of $Al_2O_3 + TiO_2$ or of $MgF_2 + CeO_2$. A significant increase in reflectance in the visible is found for aluminium mirrors coated in this way (Hass 1955).

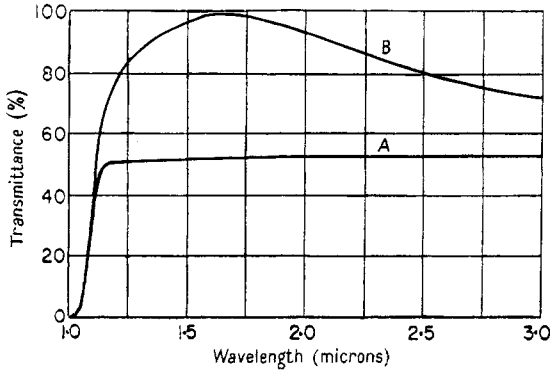

Figure 45. Si plate bloomed with SiO films. A, uncoated plate ; B, coated plate.

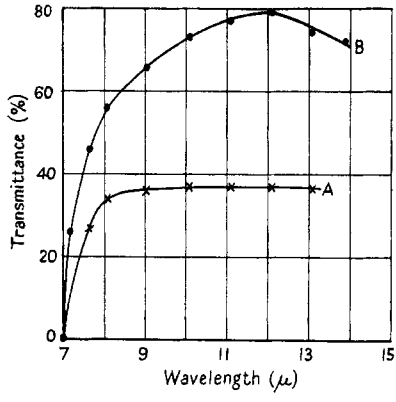

Figure 46.
InSb slab bloomed with $PbCl_2$ films.
A, uncoated plate ; B, coated plate.

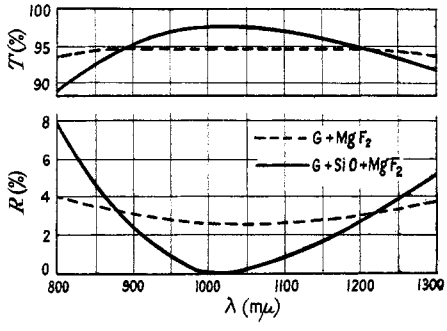

Figure 47.
Glass bloomed with one- and two-layer anti-reflecting coatings (near infra-red).

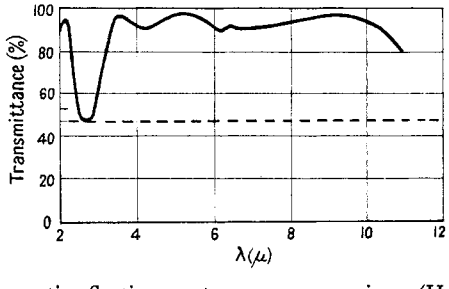

Figure 48. Three-layer anti-reflecting system on germanium (Hass and Turner 1957). Broken line, uncoated plate.

8.2.2. *Reflection filters.*

Selective reflection over a limited wavelength region may be effected by depositing interference combinations of dielectric and metal films on an opaque mirror (Hadley and Dennison 1947, 1948, Turner and Hopkinson 1953). By the use of semiconducting films which possess high absorption in the visible but are transparent in the infra-red, mirror combinations can be made which are practically non-reflecting in the visible but highly reflecting beyond about 0·8 μ. The position at which the cut-on wavelength occurs may be adjusted partly by choice of

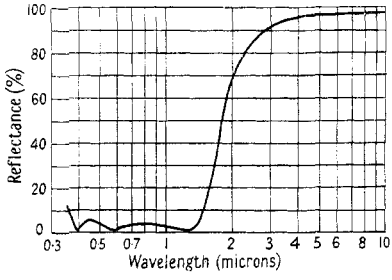

Figure 49. Reflection characteristic of dark mirror Al–SiO–Al–SiO (Hass, Schroeder and Turner 1956).

base metal and partly by the thickness of the layers. Figure 49 illustrates the type of reflectance curve which can be obtained in this way (Hass, Schroeder and Turner 1956).

For a system required to transmit visible light and reflect infra-red, stacks of non-absorbing layers may be used. Suitable designs are discussed by Epstein (1955).

8.2.3. *All-dielectric reflection systems.*

High reflectance around λ_0 is easily attained by the use of multilayer stacks of alternate $\lambda_0/4$ high- and low-index layers. Table 3 gives the calculated maximum reflectances attainable at normal incidence for three typical systems (eqn (34)).

Table 3. Calculated Reflectance at Maximum of Quarter-wave Stacks

System	CeO_2 + cryolite $\lambda = 550$ mμ	$Sb_2S_3 + CaF_2$ $\lambda = 1\ \mu$	Ge + cryolite $\lambda = 2\ \mu$
DH	0·35	0·447	0·69
DHLH	0·73	0·835	0·96
DHLHLH	0·91	0·900	$0{\cdot}99_8$
DHLHLHLH	0·97	0·977	—
	$n_D = 1{\cdot}52$	$n_D = 1{\cdot}45$	$n_D = 1{\cdot}45$

D = dielectric substrate ; H = $\lambda/4$ high-index layer ; L = $\lambda/4$ low-index layer.

The low absorption of multilayer dielectric stacks compared with that of metallic reflecting films is of considerable advantage in interferometric applications. Nine-layer ZnS + cryolite systems, with a reflectance of 97–98% in the visible, absorb less than 1%. (The loss is probably by scattering rather than by true absorption.) The application of quarter-wave multilayers to the Fabry–Perot etalon (Steudel 1957, Giacomo 1958, Ring, Beer and Hewison 1958) shows that the optical

performance of an etalon employing optical flats is limited by the irregularities of the flats. The use of a mica spacer is suggested : this makes use of the fact that certain grades of mica cleave to form parallel-sided sheets which are smooth to within one lattice spacing (~ 2 mμ).

Broad-band reflecting system. The bandwidth over which high reflectance is shown may be broadened by the use of staggered layer thicknesses. Baumeister and Stone (1956) give a simple procedure for computing the characteristics of a coating to give a broad reflectance band over the visible spectrum. The computation is performed first for a system of n layers of optical thicknesses $\lambda_i/4$ ($i = 1, 2, \ldots, n$). If we assume that, in order to get a better fit with a given reflectance curve, the thicknesses are altered by $\delta\lambda_i$, we may write for the reflectance change at any wavelength :

$$\delta R(\lambda) = \sum_n A_i(\lambda)\,\delta\lambda_i \qquad \ldots\ldots(72)$$

to first order. The $A_i(\lambda)$ are calculated, using the computer, from equation (38). $A_i(\lambda) \equiv (\partial R/\partial\lambda)_i$. From the given and approximate curves δR is read off at n wavelengths ; the computer then solves the n simultaneous equations for $\delta\lambda_i$. The process is repeated for as long as the computer is hired. The resultant reflectance

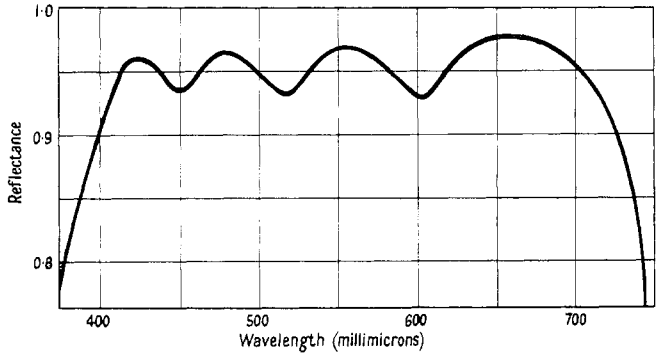

Figure 50. Broad-band reflecting multilayer systems (Baumeister and Stone 1956).

curve for a 15-layer system of $\lambda_i/4$ layers of ZnS and cryolite is shown in figure 50. The λ_i values used are given in table 4.

Table 4. Broad-band Multilayer Design : values of λ_i

Layer No.	λ_i (mμ)	Layer No.	λ_i (mμ)
1 (ZnS)	690·8	9	520·5
2 (cryl)	690·8	10	463·7
3	690·8	11	463·7
4	666·7	12	434·8
5	575·7	13	414·0
6	701·3	14	414·0
7	626·2	15	414·0
8	517·0		

Such a system exhibits a very high dispersion of phase change on reflection (Baumeister and Jenkins 1957) ; when used in an interference filter very sharp

bands result, occurring at wavelengths which are less critically dependent on the spacer thickness than in the simple all-dielectric filter.

The use of multilayers extends the limit of Fabry–Perot interferometry into the infra-red. Combination of a grating instrument with an etalon enables very high resolution to be attained. With multilayers of reflectance only 65%, Jaffe, Rank and Wiggins (1955) obtain a resolution of 0·043K at 660K. Since very much higher reflectances are now easily obtainable it is clear that this technique is capable of considerable development.

Multilayers in the ultra-violet and infra-red. There are few materials with high refractive indices which are transparent far into the ultra-violet : although suitable for the visible region, ZnS and CeO_2 begin to absorb sufficiently to make them unsuitable for multilayers at the blue end of the spectrum. Rubidium iodide and cryolite multilayers have been made by Rimbert, Lennuier and Cojan (1955) giving $R = 0{\cdot}70$ and $A = 0{\cdot}05$ at $\lambda = 250\,\mathrm{m}\mu$. Lead chloride and magnesium fluoride yield $R = 0{\cdot}94$ at wavelengths down to 300 mμ (Penselin and Steudel 1955) ; antimony oxide and cryolite are slightly better, the absorbing cut-off occurring about 8 mμ lower (Barr and Jenkins 1956). Caesium iodide with either cryolite or magnesium fluoride has been used in the region 250–280 mμ the absorption being 2·5–4% for 11 and 13 layers. Caesium bromide and cryolite can be used in the region 230–250 mμ. In these cases it is necessary to protect the soluble alkali halide films by a protective layer of NaF, MgF_2 or paraffin (Steudel and Stotz 1958).

The near infra-red is an especially favourable region since there exist several materials which have refractive indices up to about 6 and which are quite transparent. Germanium and cryolite are satisfactory beyond 1·7 μ until mechanical failure of cryolite sets in at optical thicknesses of the order of 2 μ (i.e. $\lambda/4$ at 8 μ) (Heavens, Ring and Smith 1957). Combinations of tellurium and sodium chloride have been used by Greenler (1955) yielding $R = 0{\cdot}80$ with negligible absorption in the neighbourhood of 12–15 μ.

8.3 *Interference Filters*

8.3.1. *Fabry–Perot type filter.*

The early Fabry–Perot type of interference filter consists of a dielectric spacer layer sandwiched between partly reflecting silver films, deposited on a suitable substrate. The transmission characteristic of such a filter is given approximately by the Airy summation. Maxima occur at integral multiples of wave number $\nu_0 = (2nt)^{-1}$, where n is the refractive index of the spacer and t is the effective thickness (metrical spacer thickness plus path equivalent of phase changes at the dielectric–silver interfaces). The maximum transmittance of the filter is limited by the absorption of the silver layers. The effects of absorption may be reduced by combining the silver layers with suitable multilayer dielectric stacks (Berning and Turner 1957). Considerable improvement in respect of transmittance and bandwidth is obtained by the use of high-reflecting multilayer stacks in place of the silver films. The free spectral range is less than that for the silver + dielectric system since the reflectance of the multilayer stacks decreases away from the maximum. Figure 51 compares the transmission curves for (*a*) the Airy sum, ignoring absorption and (*b*) a five-layer filter for the near infra-red using germanium

(index 4·0) and cryolite (index 1·35). The disadvantage of the limited free spectral range is not serious : the efficiency of the all-dielectric Fabry–Perot filter is so high that unwanted sidebands can easily be removed by auxiliary filtering. The ultimate performance of this type of filter appears to be limited by the inherent inhomogeneities of vacuum-deposited layers. Giacomo, Baumeister and Jenkins (1959) have investigated the effects of errors in the constituent layer thicknesses on the filter performance. The use of a mica spacer (Heavens, Ring and Smith 1957) in place of an evaporated layer leads to a better performance : control of the spacer thickness is difficult although a small range of adjustment of the passband wavelength is obtainable by tilting. Typical figures for maximum transmittance and bandwidth quoted by one manufacturer are : 95% transmittance at 5 mμ bandwidth to 80% transmittance at 1·5 mμ bandwidth (visible spectrum).

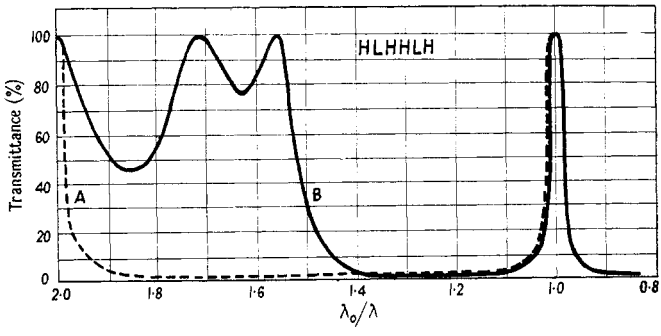

Figure 51. Comparison of Airy curve (A) with that for all-dielectric Fabry–Perot type filter (B). System HLHHLH.

For the near infra-red, filters of this type may be made for wavelengths up to about 10 μ (Greenler 1957). In the region 2–5 μ germanium and cryolite may be used ; bandwidths of the order 1·5% of the passband wavelength are obtained. With tellurium and sodium chloride at $\lambda = 10\ \mu$ a peak transmittance of 40–80% corresponding to bandwidths 0·10 μ to 0·05 μ are possible.

8.3.2. *Double and treble half-wave systems.*

The shape of the transmission band of the Fabry–Perot type of filter is not ideal since one-half of the energy transmitted at one order lies outside the filter half-width. Considerably better performance is obtained with systems of the type

$$\text{stack}/\tfrac{1}{2}\lambda/\text{stack}/\tfrac{1}{2}\lambda/\text{stack} \quad \text{(Smith 1958)}$$

and $\text{stack}/\tfrac{1}{2}\lambda/\text{stack}/\tfrac{1}{2}\lambda/\text{stack}/\tfrac{1}{2}\lambda/\text{stack}$ (Turner *et al.* 1953, Smith 1958).

The double half-wave system can yield a narrow passband such as that of figure 52 : the treble half-wave (described by Turner as a WADI—wide-band all-dielectric interference filter) can give three maxima, as shown in figure 53. At wavelengths around twice the passband wavelength, the double half-wave system may show a fairly steep rise, with continued high transmission to indefinitely long wavelengths, the limit being in practice set by the onset of absorption in the film materials.

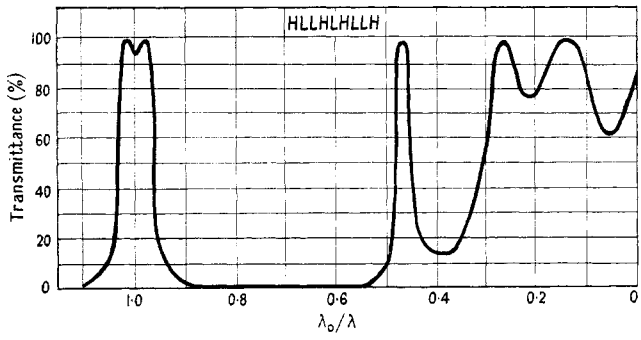

Figure 52. Transmittance characteristic of double half-wave system HLLHLHLLH.

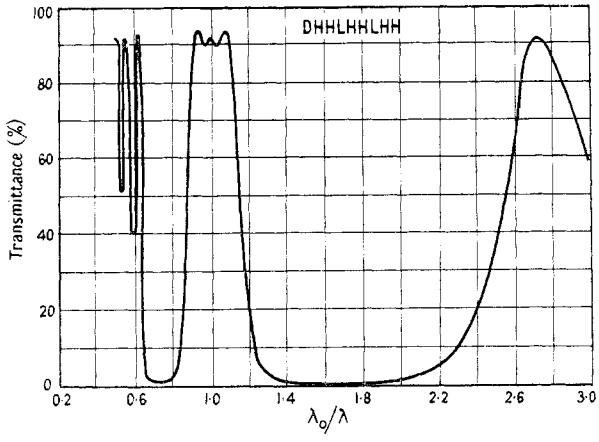

Figure 53. Transmittance characteristic of treble half-wave system DHHLHHLHH.

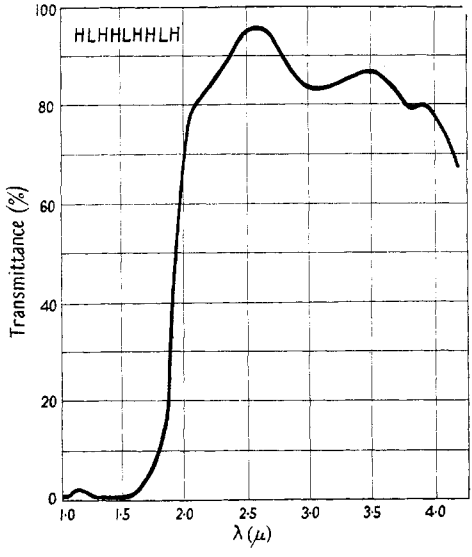

Figure 54. Experimental double half-wave filter for the near infra-red.

Experimental curves of such filters for the infra-red are shown in figure 54. This type of filter is invaluable for suppressing the high-frequency passbands characteristic of any of the narrow-band filters discussed above. The very high absorption of the semiconductor layers used ensures that no visible transmission occurs. If it is desired to cut off at long wavelengths, this can generally easily be effected by the choice of substrate.

A Fabry–Perot type of filter with a variable air-gap as the spacer layer has been constructed by Smith and Heavens (1957) which allows a passband of width of order 0·02 μ to be selected in the range 1·75 to 2·25 μ. When combined with a double half-wave cut-on filter, the transmission characteristic shown in figure 55 is obtained.

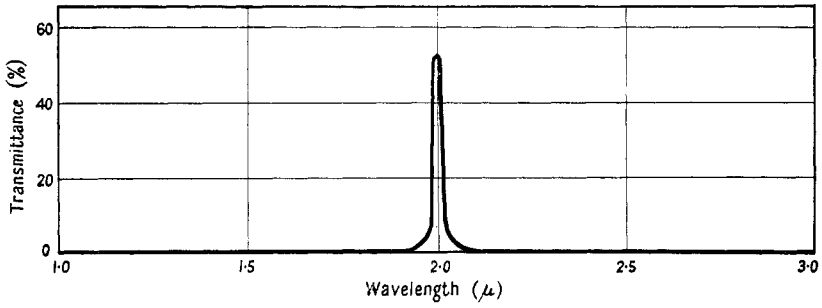

Figure 55. Experimental transmission curve for combination of Fabry–Perot filter with cut-on system. The position of the peak may be varied over $\pm 0{\cdot}25$ μ without loss of shape.

8.3.3. *The frustrated total reflection filter.*

The simple filter introduced by Turner (1950) suffers from the disadvantage of possessing two passbands, arising from the difference in phase changes on reflection of the components of different polarization. This difficulty is overcome by Billings (1950) by the use of a birefringent spacer layer, which brings the passbands together. An analysis of a seven-layer F.T.R. filter with isotropic layers by Kard (1957a) shows that the main passbands for the two components can be brought together. Since the secondary maxima for the two polarized components are found to occur at different wavelengths, these may be eliminated by the use of two such filters.

8.4 *Polarization Devices*

Thin film systems may usefully be employed in polarization devices of various kinds. Several examples have been made which illustrate their potentialities although they have not so far been widely exploited. The analogy with the pile-of-plates polarizer has the advantage that, using films of interference thicknesses, interference effects may be used to discriminate between the polarized components. Thus with two glass ($n = 1{\cdot}53$) plates coated on each side with films of TiO_2, Abelès (1950) produces a degree of polarization of 0·997 at the centre of the visible spectrum ; at the ends of the visible spectrum the degree of polarization is still as high as 0·993. The use of multilayers on a prism face to produce a beam-splitter, described by Banning (1947), enables an average degree of polarization of 0·98 to be

obtained over the visible spectrum for a range of angle of incidence $\pm 5°$ from normal.

The use of thin dielectric films deposited on a totally reflecting prism face, for the production of quarter- and half-wave plates has been examined by Lostis (1959). A single reflection at the hypotenuse of a 45° prism ($n = 1{\cdot}52$) coated with a layer of CeO_2 ($n = 2{\cdot}1$) of thickness $\lambda/3$ produces a relative phase difference of 90°. Over the visible spectrum the variation of the phase difference introduced lies within $\pm 6{\cdot}5°$ of the exact $\lambda/4$ value. For a half-wave layer a film of thickness 0·92 and of index 2·6 is required (TiO_2): in this case the variation over the visible spectrum is $\pm 5°$. Calculations of the dependence of the relative phase difference on film thickness (eqn (27)) show that the performance of such systems is not critically dependent on this quantity.

8.5 *Heat Absorbing Systems*

Systems which absorb nearly the whole of the incident radiation energy are of interest and importance as radiation detectors. A single unsupported metal film absorbs a maximum of 50%, transmitting and reflecting 25% of the incident energy. Systems of three layers—metal/dielectric/metal—have been examined by

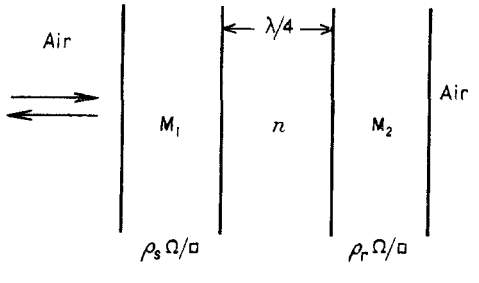

Figure 56.

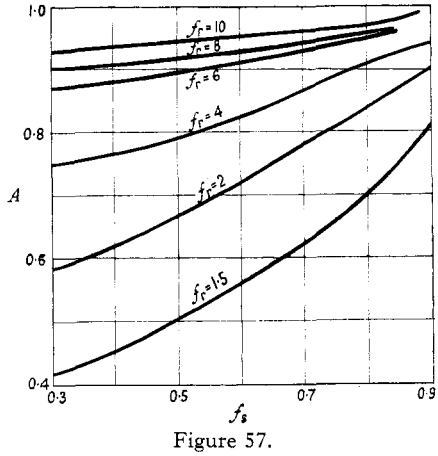

Figure 57.

Hilsum (1954) and Silberg (1957) and are shown to be capable of absorbing up to about 95% of the incident radiation. For normal incidence on the system of figure 56 the absorption is given by

$$A = \frac{4f_s(f_r+1)^2+f_r n^2}{[(f_s+1)(f_r+1)+n^2]^2} \qquad \ldots\ldots(73)$$

where $f_i = 377/\rho_i$ and ρ_i is the resistance of the film in ohms per square. Maximum absorption is obtained for

$$n = \frac{(f_r+1)(1-f_s)^{1/2}}{(f_r-1)^{1/2}} \qquad \ldots\ldots(74)$$

for $0 < f_s < 1$ and $f_r > 1$. Figure 57 shows the values of A obtainable for various values of f_r and f_s. For $f_r = 10$ and $f_s = 0{\cdot}8$ the value of n required is approximately 1·5. These values are easily realized in practice.

APPENDIX I

Refractive Indices of Transparent Materials in Thin Film Form

In the table below are collected values obtained for refractive indices of films, formed by thermal evaporation unless otherwise stated. In many cases the actual index depends markedly on the conditions of preparation. Where the effects are known these are mentioned. Values of n are given generally for a wavelength near the centre of the visible spectrum. All the materials listed which are transparent in the visible spectrum show normal dispersion. Where detailed information is available on the dispersion, the appropriate references will be found in § 6. An indication is given of the range of wavelength over which the materials are usable in multilayer systems.

Substance	Refractive index	Wavelength (mμ)	Range of transparency from	to	Remarks
CaF_2	1·23–1·26	546	< 150 mμ	15 μ	Poor vacuum
CaF_2	1·36	white			
NaF	1·34	589	< 250 mμ		Bulk index
LiF	1·36–1·37	546	< 110 mμ	10 μ	
Cryolite	1·35–1·39	570	< 200 mμ	10 μ	
AlF_3	1·38–1·39	546			
MgF_2	1·39–1·40	546	230 mμ	10 μ	Aged films
SiO_2	1·44		200 mμ	5 μ	
ThF_4	1·45			> 10 μ	
NaCl	1·54	589	< 200 mμ	> 15 μ	Not water-grown crystals
KBr	1·56	589	600 mμ	30 μ	Not water-grown crystals
$CaSiO_3$	1·68	550			
WO_3	1·8			> 10 μ	
CsBr	1·8		230 mμ	40 μ	
SiO	1·55 to 2·00	vis.	500 mμ	8 μ	Slowly evaporated Rapidly evaporated
Tin oxide	1·96			> 10 μ	
MoO_3	2·0				
CsI	2·0	u. v.	250 mμ	750 μ	
RbI	2·0	u. v.	250 mμ		
Sb_2O_3	2·1	u. v.	290 mμ		
$PbCl_2$	2·0	10 μ	300 mμ	> 14 μ	
	2·2	300 mμ			
Anodic Ta_2O_5	2·20	590 mμ			
ZnS	2·37	546 mμ	400 mμ	14 μ	
Anodic TiO_2	2·40	546 mμ			
CeO_2	2·42	550 mμ			Rapid deposition
Se	2·5		700 mμ	20 μ	
CdS	2·5–2·7	500 mμ	520 mμ	> 14 μ	
Thermal TiO_2	2·73	546 mμ			
Sb_2S_3	3·0	589 mμ	500 mμ	10 μ	
Si	3·5		> 1 μ		
InSb	4·0		3–7 μ		Depends on purity
PbS	4·0	3 μ	3 μ		
Ge	4·3–4·6	2 μ	1·7 μ	20 μ	
Te	4·9	6 μ	3·4 μ	20 μ	
PbSe					
PbTe	5·5		3·8 μ		
Barium stearate	1·49–1·50	white			Deposited from trough by Blodgett technique
Stearic acid	1·54	white			Deposited from trough by Blodgett technique
Haemine	$n = 1·7$, $k = 0·30$	425			Monomolecular layers, 2 mμ thick (Lostis 1955)

APPENDIX II

Optical Constants of Opaque Metal Films

Alkali Metals

Measurements made at the quartz–metal interface of films formed by evaporation and subsequently re-melted *in vacuo* between the quartz plates. No details available on pressure in system. The action of re-melting presumably results in a layer with substantially the bulk properties (Ives and Briggs 1936, 1937 a, b).

Wavelength	Sodium		Potassium		Rubidium		Caesium	
(mμ)	*n*	*k*	*n*	*k*	*n*	*k*	*n*	*k*
253·6	0·026	0·62	0·744	0·049	1·031	0·056	0·916	0·143
312·6	0·040	1·02	0·410	0·080	0·814	0·078	0·827	0·174
365·0	0·042	1·44	0·150	0·443	0·496	0·135	0·671	0·233
404·7	0·048	1·56	0·105	0·710	0·275	0·373	0·540	0·320
435·8	0·048	1·80	0·121	0·978	0·181	0·636	0·425	0·438
546·1	0·029	2·32	0·091	1·42	0·157	1·05	0·278	0·950
578·0	0·027	2·59	0·094	1·57	0·164	1·19	0·264	1·123

Thick Annealed Films of Ag, Au, Cu and Al

Measurements by Schulz using the methods given in §5.2.5. The films are annealed until, by the $R_s^2 = R_p$ criterion, they are homogeneous.

Wavelength	Silver		Gold		Copper		Aluminium	
(mμ)	*n*	*k*	*n*	*k*	*n*	*k*	*n*	*k*
400	0·075	1·93	1·45		0·85		0·40	3·92
450	0·055	2·42	1·40	1·88	0·87	2·20	0·49	4·32
500	0·050	2·87	0·84	1·84	0·88	2·42	0·62	4·80
550	0·055	3·32	0·34	2·37	0·72	2·42	0·76	5·32
600	0·060	3·75	0·23	2·97	0·17	3·07	0·97	6·00
650	0·070	4·20	0·19	3·50	0·13	3·65	1·24	6·60
700	0·075	4·62	0·17	3·97	0·12	4·17	1·55	7·00
750	0·080	5·05	0·16	4·42	0·12	4·62	1·80	7·12
800	0·090	5·45	0·16	4·84	0·12	5·07	1·99	7·05
850	0·100	5·85	0·17	5·30	0·12	5·47	2·08	7·15
900	0·105	6·22	0·18	5·72	0·13	5·86	1·96	7·70
950	0·110	6·56	0·19	6·10	0·13	6·22	1·75	8·50

Optical Constants of Ag, Pb and Sn in the Near Infra-red
(Motulevich and Shubin 1957)

λ(μ)	Silver		Lead		Tin	
	n	*k*	*n*	*k*	*n*	*k*
1·03	0·27	7·00	—	—	—	—
1·28	0·36	8·58	1·55	7·0	3·7	8·1
1·71	0·53	11·7	2·1	9·7	3·0	10·7
2·50	0·91	17·2	3·55	14·0	3·6	15·7
3·48	1·65	23·75	5·75	18·5	5·7	20·9
4·38	2·0	29·65	8·0	22·4	6·9	25·2
5·38	2·9	36·9	10·5	26·4	9·0	30·0
6·00	4·3	40·65	12·5	26·8	10·0	32·0
7·09	—	—	12·6	29·5	11·2	34·5

No information on film structure.

References

Abelès, F., 1948 a, *Ann. Phys., Paris*, **3**, 504 ; 1948 b, *C.R. Acad. Sci., Paris*, **226**, 1808 ; 1950, *J. Phys. Radium*, **11**, 310, 403.

Alderson, R. H., and Ashworth, F., 1957, *Brit. J. Appl. Phys.*, **8**, 205.

Avery, D. G., 1950, *Phil. Mag.*, **41**, 1018.

Bailly, R., 1938, *Bull. Cl. Sciences Belg.*, **24**, 791.

Banning, M., 1947, *J. Opt. Soc. Amer.*, **37**, 688, 792.

Bannon, J., 1946, *Nature, Lond.*, **157**, 446.

Barr, W. L., and Jenkins, F. A., 1956, *J. Opt. Soc. Amer.*, **46**, 141.

Baumeister, P. W., and Jenkins, F. A., 1957, *J. Opt. Soc. Amer.*, **47**, 57.

Baumeister, P. W., and Stone, J. M., 1956, *J. Opt. Soc. Amer.*, **46**, 228.

Beattie, J. R., 1955, *Phil. Mag.*, **46**, 235.

Beattie, J. R., and Conn, G. K. T., 1955, *Phil. Mag.*, **46**, 989.

Belk, J. A., Tolansky, S., and Turnbull, D., 1954, *J. Opt. Soc. Amer.*, **44**, 5.

Berning, P. H., 1956, *J. Opt. Soc. Amer.*, **46**, 779.

Berning, P. H., and Turner, A. F., 1957, *J. Opt. Soc. Amer.*, **47**, 230.

Billings, B. H., 1950, *J. Opt. Soc. Amer.*, **40**, 471.

Billings, B. H., and Hyman, M., 1947, *J. Opt. Soc. Amer.*, **37**, 119.

Blaisse, B. S., 1950, *J. Phys. Radium*, **11**, 315.

Blodgett, K. B., and Langmuir, I., 1937, *Phys. Rev.*, **51**, 964.

Bor, J., and Chapman, B. G., 1949, *Nature, Lond.*, **157**, 182.

Bousquet, P., 1956, *Opt. Acta*, **3**, 153 ; 1957, *Ann. Phys., Paris*, **2**, 5.

Bousquet, P., and Delcourt, Y., 1957, *J. Phys. Radium*, **18**, 447.

Bradley, R. S., 1953, *J. Sci. Instrum.*, **30**, 84.

Charlesby, A., and Polling, J. J., 1955, *Proc. Roy. Soc.* A, **227**, 434.

Clegg, P. L., 1952, *Proc. Phys. Soc.* B, **65**, 774.

Clegg, P. L., and Crook, A. W., 1952, *J. Sci. Instrum.*, **29**, 201.

Coogan, C. K., 1957, *Proc. Phys. Soc.* B, **70**, 845.

Cotton, P., 1950, *J. Phys. Radium*, **11**, 375.

Cox, J. T., and Hass, G., 1958, *J. Opt. Soc. Amer.*, **48**, 677.

Cox, J. T., Hass, G., and Rowntree, R. F., 1954, *Vacuum*, **4**, 445.

Crook, A. W., 1948, *J. Opt. Soc. Amer.*, **38**, 954.

David, E., 1939, *Z. Phys.*, **114**, 389.

Dingle, R. B., 1953, *Physica*, **19**, 729.

Ditchburn, R. W., 1952, *Light* (London : Blackie).

Ditchburn, R. W., and Orchard, G. A. J., 1954, *Proc. Phys. Soc.* B, **67**, 608.

Drude, P., 1891, *Wied. Ann.*, **43**, 146.

Dumontet, P., Perrot, M., and Tortosa, J., 1957, *C.R. Acad. Sci., Paris*, **244**, 2488.

Duncan, R. W., and Duncan, R. C., 1913, *Phys. Rev.*, **1**, 294.

Dyson, J., 1958, *Physica*, **24**, 532.

Epstein, L. I., 1952, *J. Opt. Soc. Amer.*, **42**, 806 ; 1955, *Ibid.*, **45**, 360.

Ewald, P., 1916, *Ann. Phys., Lpz.*, **49**, 117.

Fabre, D., and Romand, J., 1956, *C.R. Acad. Sci., Paris*, **242**, 893.

Faust, R. C., 1950, *Phil. Mag.*, **41**, 1238.

Fochs, P. D., 1950, *J. Opt. Soc. Amer.*, **40**, 623.

Försterling, K., 1937, *Ann. Phys., Lpz.*, **30**, 745.

Försterling, K., and Fréedericksz, V., 1913, *Ann. Phys., Lpz.*, **40**, 201.

Françon, M., 1952, *Rev. Opt.*, **31**, 65 ; 1953, *Ibid.*, **32**, 349 ; 1954, *Opt. Acta*, **1**, 50.

Frau, C., 1952, *Rev. Opt.*, **31**, 161.

Garnett, J. C. M., 1904, *Phil. Trans. Roy. Soc.*, **203**, 385 ; 1906, *Ibid.*, **205**, 237.

Gates, D. M., Shaw, C. C., and Beaumont, D., 1958, *J. Opt. Soc. Amer.*, **48**, 88.

van Geel, W. C., and Schelen, B. J. J., 1957, *Philips Res. Rep.*, **12**, 240.

Gerharz, R., 1958, *Z. Angew. Phys.*, **9**, 95.

Giacomo, P., 1958, *J. Phys. Radium*, **19**, 307.

Giacomo, P., Baumeister, P. W., and Jenkins, F. A., 1959, *Proc. Phys. Soc.*, **73**, 480.

GIACOMO, P., and JACQUINOT, P., 1952, *J. Phys. Radium*, Suppl. No. 2, 59A.
GILLHAM, E. J., PRESTON, J. S., and WILLIAMS, B. E., 1955, *Phil. Mag.*, **46**, 1051.
GODFREY, G. H., 1957, *Austral. J. Phys.*, **10**, 1.
GRARD, F., 1957 a, *Bull. Cl. Sciences Belg.*, **43**, 641 ; 1957 b, *J. Phys. Radium*, **17**, 414 ; 1957 c, *Bull. Cl. Sciences Belg.*, **43**, 628.
GREENLER, R. G., 1955, *J. Opt. Soc. Amer.*, **45**, 788 ; 1957, *Ibid.*, **47**, 130.
HADLEY, L. N., and DENNISON, D. M., 1947, *J. Opt. Soc. Amer.*, **37**, 451 ; 1948, *Ibid.*, **38**, 483.
HALL, J. F., 1956, *J. Opt. Soc. Amer.*, **46**, 1013 ; 1957, *Ibid.*, **47**, 662.
HALL, J. F., and FERGUSON, W. F., 1955 a, *J. Opt. Soc. Amer.*, **45**, 74 ; 1955 b, *Ibid.*, **45**, 714.
HAMMER, K., 1943, *Z. Tech. Phys.*, **24**, 169.
HARRIS, L., 1955, *J. Opt. Soc. Amer.*, **45**, 27.
HARRIS, L., and LOEB, A. L., 1955, *J. Opt. Soc. Amer.*, **45**, 179.
HARTMAN, R. E., 1954, *J. Opt. Soc. Amer.*, **44**, 192.
HARTMAN, R. E., HARTMAN, R. S., LARSON, K., and BATEMAN, J. B., 1954, *J. Opt. Soc. Amer.*, **44**, 197.
HASS, G., 1949, *J. Opt. Soc. Amer.*, **39**, 532 ; 1952, *Vacuum*, **2**, 331 ; 1955, *J. Opt. Soc. Amer.*, **45**, 945.
HASS, G., HUNTER, W. R., and TOUSEY, R., 1956, *J. Opt. Soc. Amer.*, **46**, 1009 ; 1957, *Ibid.*, **47**, 1070.
HASS, G., RAMSEY, J. B., and THUN, R., 1958, *J. Opt. Soc. Amer.*, **48**, 324.
HASS, G., and SALZBURG, C. D., 1954, *J. Opt. Soc. Amer.*, **44**, 181.
HASS, G., SCHROEDER, H. H., and TURNER, A. F., 1956, *J. Opt. Soc. Amer.*, **46**, 31.
HASS, G., and TURNER, A. F., 1957, *Ergebnisse der Hochvacuumtechnik und der Physik dünner Schichten* (Stuttgart : Wissenschaftliche Verlagsgesellschaft).
HEAVENS, O. S., 1951, *Proc. Phys. Soc.* B, **64**, 419 ; 1955, *Optical Properties of Thin Solid Films* (London : Butterworths Scientific Publications) ; 1959, *Lab. Pract.*, in the press.
HEAVENS, O. S., and KELLY, J. C., 1958, *Proc. Phys. Soc.*, **72**, 906 ; 1959, *Opt. Acta*, **6**, 339.
HEAVENS, O. S., RING, J., and SMITH, S. D., 1957, *Spectrochim. Acta*, **10**, 179.
HEAVENS, O. S., and SMITH, S. D., 1957, *J. Opt. Soc. Amer.*, **47**, 469.
VAN HEEL, A. C. S., and WALTHER, A., 1958, *Opt. Acta*, **5**, 47.
HERMANSEN, A., 1955, *K. Danske Vidensk. Selsk., Mat.-Fys. Medd.*, **30**, No. 6.
HERPIN, A., 1947, *C.R. Acad. Sci., Paris*, **225**, 182.
HILSUM, C., 1954, *J. Opt. Soc. Amer.*, **44**, 188.
HODGSON, J. N., 1955, *Proc. Phys. Soc.* B, **68**, 593.
HOLLAND, L., and SIDDALL, G., 1953, *Vacuum*, **3**, 375.
HULDT, L., and STAFLIN, T., 1959, *Opt. Acta*, **6**, 27.
HUTCHINSON, A., 1907, *Min. Mag.*, **14**, 199.
IVES, H. E., and BRIGGS, H. B., 1936, *J. Opt. Soc. Amer.*, **26**, 238 ; 1937 a, *Ibid.*, **27**, 395 ; 1937 b, *Ibid.*, **27**, 181.
JAFFE, J. H., RANK, D. H., and WIGGINS, T. A., 1955, *J. Opt. Soc. Amer.*, **45**, 636.
JARRETT, A. H., 1952, *Nature, Lond.*, **169**, 790.
JENESS, J. R., 1956, *J. Opt. Soc. Amer.*, **46**, 157.
JOHNSON, W. C., 1955, *Organic Reagents for Metals* (London : Hopkins and Williams).
KANDARE, S., and FABRE, D., 1956, *C.R. Acad. Sci., Paris*, **242**, 1150.
KARD, P. G., 1956, *Soviet Physics, Doklady*, **1**, 256 ; 1957 a, *Izvest. Akad. Nauk Eston., S.S.S.R.*, **6**, 344 ; 1957 b, *Opt. i Spekt.*, **2**, 236, 245.
KELLY, J. C., 1958 a, *Opt. Acta*, **5**, 75 ; 1958 b, *Ph.D. Thesis*, University of Reading.
KOEHLER, W. F., 1953, *J. Opt. Soc. Amer.*, **43**, 738 ; 1955, *Ibid.*, **45**, 943.
KRAUS, H. L., 1949, *Elect. Engng*, **68**, 767.
KRAUTKRÄMER, J., 1938, *Ann. Phys., Lpz.*, **32**, 537.
KRONIG, R. DE L., 1931, *Proc. Roy. Soc.* A, **133**, 255.
KRYLOVA, T. N., 1958, *Opt. i Spekt.*, **4**, 217.
KUNZE, C., 1958, *Ann. Phys., Lpz.*, [7], **1**, 165.
KUWABARA, G., and ISIGURO, K., 1952, *J. Phys. Soc. Japan*, **7**, 72.
LEBERKNIGHT, C. E., and LUSTMAN, B., 1939, *J. Opt. Soc. Amer.*, **29**, 59.

LISITSA, M. P., and TSVELYKH, N. G., 1957, *Opt. i Spekt.*, **2**, 674.
LISSBERGER, P. H., and RING, J., 1955, *Opt. Acta*, **2**, 42.
LOCKHART, L. B., and KING, P., 1947, *J. Opt. Soc. Amer.*, **37**, 689.
LOSTIS, P., 1955, *C.R. Acad. Sci., Paris*, **240**, 2130; 1959, *Rev. Opt.*, **38**, 1.
MCLAURIN, R. C., 1905, *Proc. Roy. Soc.* A, **76**, 149.
MALÉ, D., 1950, *J. Phys. Radium*, **11**, 332; 1952, *Thèse*, Université de Paris.
MALÉ, D., and ROUARD, P., 1953, *J. Phys. Radium*, **14**, 584.
MALÉ, D., and TROMPETTE, J., 1957, *J. Phys. Radium*, **18**, 128.
MATTUCK, R. D., 1956, *J. Opt. Soc. Amer.*, **46**, 615, 621.
MATTUCK, R. D., PETTI, R. D., and BATEMAN, J. B., 1956, *J. Opt. Soc. Amer.*, **46**, 782.
MAYER, H., 1950, *Physik dünner Schichte* (Stuttgart: Wissenschaftliche Verlagsgesellschaft).
MORITA, N., 1956, *J. Phys. Soc. Japan*, **11**, 957; 1957, *Ibid.*, **12**, 1142.
MOTULEVICH, G. P., and SHUBIN, A. A., 1957, *Opt. i Spekt.*, **2**, 633.
MUCHMORE, R., 1948, *J. Opt. Soc. Amer.*, **38**, 20.
MURMANN, H., 1933, *Z. Phys.*, **80**, 161; 1936, *Ibid.*, **101**, 643.
MURRAY, A. E., 1956, *J. Opt. Soc. Amer.*, **46**, 790.
O'BRYAN, H. M., 1936, *J. Opt. Soc. Amer.*, **26**, 122.
PENSELIN, S., and STEUDEL, A., 1955, *Z. Phys.*, **142**, 21.
PHILIP, R., 1956, *C.R. Acad. Sci., Paris*, **243**, 365.
PHILIP, R., and TROMPETTE, J., 1957, *J. Phys. Radium*, **18**, 92.
RANK, D. H., and BENNETT, H. E., 1955, *J. Opt. Soc. Amer.*, **45**, 69.
REIMER, L., 1957, *Optik*, **14**, 83.
REUTER, G. E. H., and SONDHEIMER, E. H., 1948, *Proc. Roy. Soc.* A, **195**, 336.
RIMBERT, G., LENNUIER, R., and COJAN, J.-L., 1955, *C.R. Acad. Sci., Paris*, **241**, 1560.
RING, J., BEER, R., and HEWISON, V., 1958, *J. Phys. Radium*, **19**, 321.
ROOD, J. L., 1949, *J. Opt. Soc. Amer.*, **39**, 854.
ROTHEN, A., 1945, *Rev. Sci. Instrum.*, **16**, 26.
ROTHEN, A., and HANSON, M., 1949, *Rev. Sci. Instrum.*, **20**, 66.
ROUARD, P., 1937, *Ann. Phys., Paris*, **7**, 291.
ROUARD, P., MALÉ, D., and TROMPETTE, J., 1953, *J. Phys. Radium*, **14**, 587.
SANDELL, E. B., 1944, *Colorimetric Determination of Traces of Metals* (New York: Interscience).
SANFORD, B. P., 1958, *J. Opt. Soc. Amer.*, **48**, 482.
SCHOPPER, H., 1951, *Z. Phys.*, **130**, 565; 1952 a, *Ibid.*, **132**, 146; 1952 b, *Ibid.*, **131**, 215.
SCHULZ, L. G., 1949, *J. Chem. Phys.*, **17**, 1153; 1950, *J. Opt. Soc. Amer.*, **40**, 690; 1951, *Ibid.*, **41**, 261; 1954 a, *Ibid.*, **44**, 357; 1954 b, *Ibid.*, **44**, 540; 1957, *Advanc. Phys.* (*Phil. Mag.* Suppl.), **6**, 102.
SCHULZ, L. G., and SCHEIBNER, E. J., 1950, *J. Opt. Soc. Amer.*, **40**, 761.
SCHULZ, L. G., and TANGHERLINI, F. R., 1954, *J. Opt. Soc. Amer.*, **44**, 362.
SCOTT, G. D., MCLAUCHLAN, T. A., and SENNETT, R. S., 1950, *J. Appl. Phys.*, **21**, 843.
SENNETT, R. S., and SCOTT, G. D., 1950, *J. Opt. Soc. Amer.*, **40**, 203.
SHALIMOVA, K. V., 1951, *Dokl. Akad. Nauk, S.S.S.R.*, **80**, 587.
SILBERG, P. A., 1957, *J. Opt. Soc. Amer.*, **47**, 575.
SINELNIKOV, K. D., SHKLIAREVSKY, I. N., and VLASENKO, N. A., 1957, *Opt. i Spekt.*, **2**, 651.
SIVUKHIN, D. V., 1956, *Soviet Physics, JETP*, **3**, 269.
SMITH, S. D., 1958, *J. Opt. Soc. Amer.*, **48**, 43.
SMITH, S. D., and HEAVENS, O. S., 1957, *J. Sci. Instrum.*, **34**, 492.
SMITH, S. D., and MOSS, T. S., 1958, *J. Sci. Instrum.*, **35**, 105.
STEUDEL, A., 1957, *Naturwissenschaften*, **44**, 249.
STEUDEL, A., and STOTZ, S., 1958, *Z. Phys.*, **151**, 233.
STRACHEN, C., 1933, *Proc. Camb. Phil. Soc.*, **29**, 116.
SUKHANOVSKY, V. V., 1956, *Dokl. Akad. Nauk, S.S.S.R.*, **106**, 226.
THELEN, A., 1956, *Optik*, **13**, 537.
TOLANSKY, S., 1948, *Multiple Beam Interferometry* (Oxford: University Press); 1951, *J. Electrodep. Tech. Soc.*, **27**, 1.
TRAUB, A. C., 1956, *J. Opt. Soc. Amer.*, **46**, 999.
TRAUB, A. C., and OSTERBERG, H., 1957, *J. Opt. Soc. Amer.*, **47**, 62.

TROMPETTE, J., 1959, *C.R. Acad. Sci., Paris*, **248**, 207.
TURNER, A. F., 1950, *J. Phys. Radium*, **11**, 444.
TURNER, A. F., and HOPKINSON, H. R., 1953, *J. Opt. Soc. Amer.*, **43**, 819.
TURNER, A. F., *et al.*, 1953, *Infra-red Transmission Filters*, Bausch and Lomb Technical Reports, Nos. 1–6.
VAŠÍČEK, A., 1940, *Phys. Rev.*, **57**, 925 ; 1947, *J. Opt. Soc. Amer.*, **37**, 145 ; 1950, *J. Phys. Radium*, **11**, 342 ; 1951, *Act. Acad. Sci. Nat., Moravo-Silesiacae*, **23**, 355.
VASILKOVSKY, A. A., 1957, *Opt. i Spekt.*, **2**, 229.
WEAVER, C., and BENJAMIN, P., 1956, *Nature, Lond.*, **177**, 1030.
WEINSTEIN, W., 1947, *J. Opt. Soc. Amer.*, **37**, 576 ; 1954, *Vacuum*, **4**, 3.
WEISS, K., 1948, *Z. Naturf.*, **3a**, 143.
WEISSKIRCHNER, W., 1951, *Z. Naturf.*, **6a**, 509.
WINTERBOTTOM, A. B., 1946, *Trans. Farad. Soc.*, **42**, 487.
WOLTER, H., 1937, *Z. Phys.*, **105**, 269.
YOUNG, L., 1958, *Proc. Roy. Soc.* A, **244**, 41.
YOUNG, N. O., and KOWAL, J., 1959, *Nature, Lond.*, **183**, 104.